A MAJOR PROJECT REPORT ON

AN OPTIMIZED HYBRID SPACE VECTOR PULSE WIDTH MODULATION FOR REDUCTION OF TORQUE RIPPLE IN VOLTAGE SOURCE INVERTER FED INDUCTION MOTOR

Submitted in *partial fulfilment of the*

Requirements for the award of the degree

of

MASTER OF TECHNOLOGY

In

POWER SYSTEMS

By

T. BHARATHA REDDY

ROLL NO. 03/P.Sy/09

Under the Guidance

Of

SUDARSHAN K.VALLURU

Associate Professor,
Department of Electrical Engineering

Department of Electrical Engineering
Delhi Technological University
Delhi-110042
2009-11

Department of Electrical Engineering

Delhi Technological University

(Formerly Delhi College of Engineering)

CERTIFICATE

This is to certify that T. Bharatha Reddy, RollNo:03/P.Sy/09,student of M.Tech, Power Systems, Department of Electrical Engineering, Delhi Technological University has submitted the dissertation entitled "AN OPTIMIZED HYBRID SPACE VECTOR PULSE WIDTH MODULATION FOR REDUCTION OF TORQUE RIPPLE IN VOLTAGE SOURCE INVERTER FED INDUCTION MOTOR" under my guidance towards partial fulfillment of the degree of M.Tech, Power Systems. This dissertation is a bonafied record of project work carried out by him under my guidance and supervision during the academic session 2010-2011.

SUDARSHAN K.VALLURU
Associate Professor
Electrical Engineering
Delhi Technological University

Prof. NARENDRA KUMAR
Head of the Department
Electrical Engineering
Delhi Technological University

ACKNOWLEDGEMENT

I wish to express my profound sense of deepest gratitude to my guide and motivator **Sudarshan K. Valluru**, Associate Professor, Electrical Engineering Department, for his valuable guidance, co-operation and finally help for providing necessary facilities and sources during the entire period of this project.

I wish to convey my gratitude to Shiva Suman, Assistant Professor, Electrical Engineering Department, for his valuable suggestions. I am thankful to the HOD and all the faculty members of Electrical Engineering Department who have enlightened me during my studies

I am grateful to my parents for their moral support all the time; they have been always around to cheer me up, in the odd times of this work. I am also thankful to my friends for their unconditional support and motivation during this work.

T.BHARATHA REDDY

M.Tech, Power Systems
Electrical Engineering Dept.
Roll no:03/P.Sy/09

ABSTRACT

The Pulse Width Modulated adjustable speed drive is popular in many new industrial applications where it desire superior performance. Recent developments in fast switching semiconductor devices have lead to improve the modulated power in three phase voltage source inverter with adjustable voltage and frequency to asynchronous motor. The most commonly used PWM schemes for three phase voltage source inverter to obtain adjustable voltage and frequency are carrier-based sinusoidal PWM and space vector PWM (SVPWM). The hybrid space vector pulse width modulation (HSVPWM) is one of the modified versions of space vector PWM.

This thesis aims to design hybrid space vector pulse width modulating technique which is combination of continuous and bus clamping pulse width modulation techniques used in voltage source inverter fed induction motor. In continuous modulation such as Conventional Space Vector Pulse Width Modulating (CSVPWM) technique, both the zero states (0 0 0) $\mathbf{V_0}$ and (1 1 1) $\mathbf{V_7}$ applied in every sub cycle, but in bus clamping PWM methods uses only one zero state in every sub cycle. This thesis also suggests certain novel switching sequences involving division of active vector time for hybrid space vector based PWM generation in voltage source inverter fed induction motor. These switching techniques implemented in MATLAB simulation and observed improvement in performance of hybrid space vector PWM, resulted in reduction of torque ripples.

Table of Contents

LIST OF FIGURES

LIST OF TABLES

NOMENCLATURE

ABBREVIATION	ACRONYM
VSI	Voltage Source Inverter
CSVPWM	Conventional Space Vector Pulse Width Modulation
HSVPWM	Hybrid Space Vector Pulse Width Modulation
SPWM	Sine Pulse Width Modulation
PWM	Pulse Width Modulation
RTRHPWM	Reduced Torque Ripple Hybrid Pulse Width Modulation
RMS	Root Mean Square
SPDT	Single Pole Double Throw
SVPWM	Space Vector Pulse Width Modulation.
THD	Total Harmonic Distortion

SYMBOLS	DESCRIPTION
f_s	Switching frequency
f	Frequency
I_{rms}	Supply RMS current
I_m	Harmonic current
M	Modulation Index
P	Poles
T_s	Switching time
Te,	Electromagnetic torque
T_L	Load torque
T_1,T_2,T_z	Switching times
T_{an}, T_{bn}, T_{cn}	Imaginary switching times
V_{in}	Input voltage
V_{ref}	Reference voltage
V/f	Voltage/Frequency
V_s	Space vector
V_d	d-axis voltage vector
V_q	q-axis voltage vector
V_{ao}, V_{bo}, V_{co}	Pole voltages of a, b, c
V_{an}, V_{bn}, V_{cn}	Phase voltages of a, b, c

CHAPTER -1

INTRODUCTION

1.1 Background

In the early decades of the twentieth century the constant frequency constant voltage magnitude balanced three-phase AC power source was found to be the most economical for the generation, transmission and distribution .Therefore, industrial consumer have been supplied with three phase AC power sources through large power grids and inter-ties even located at far-flung areas. However, it has been long recognized this form of power is not suitable for many industrial applications, which require adjustable voltage source, and most of the AC motors requires three phase alternating voltage with adjustable frequency and magnitude. Therefore, in most of industrial applications, the utility of adjustable power requires interfacing devices to convert fixed power. The strong demand for power conversion and conditioning devices to achieve these tasks has lead to the establishment of the power electronics field early this century. High performance semiconductors power switches, efficient power converter circuit topologies, and intelligent control algorithms have been developed. As a result of this development, today's industrial loads are connected to the AC power line through cost effective power converter circuits which enhance the overall performance, efficiency and reliability.

Out Of all the modern power electronics converters, the Voltage Source Inverter (VSI) is most widely used with low power to high power ranging. It converts a fixed DC voltage to the three phase AC voltages with adjustable frequency and magnitude [1]-[4].

1.2 Harmonics

The supply harmonics are causes to develop torque ripples and current ripples in an induction motor. The pure sine wave do not contain harmonics called fundamental wave as shown in fig 1.1(a), and introduction of odd harmonics causes the fundamental wave was distorted as shown in fig 1.1(b) and (c). If more number of odd harmonics are introduced, the fundamental wave was corrupted and similar to distorted square wave shown in fig 1.1(d).

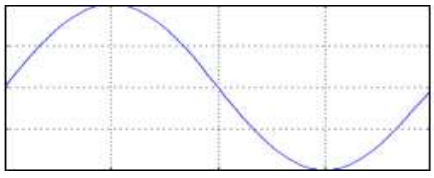

. **(a)**

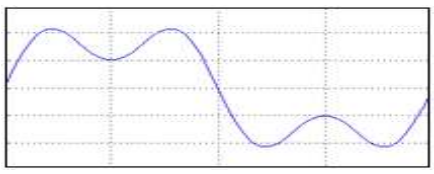

(b)

(c) **(d)**

Figure 0.1 Harmonic Estimation

The torque produced in a VSI fed induction motor is proportional to square of VSI output voltage.

$$T \ \alpha \quad (V_{in})^2 \qquad (1.1a)$$

In adjustable speed drives are fed by converters, which contain harmonics at the output, These time harmonics have shown effects in torque pulsation and heating [5]-[10]. The time harmonics in the applied voltage, results increases the losses in the motor. The harmonic currents are responsible for producing speed and torque ripple in the motor [11]. The Fourier series expression for the voltage supplied to the motor is

$$V_{in} = \sqrt{2}\,(V_1 \sin\omega t + V_3 \sin 3\omega t + V_5 \sin 5\omega t + v_7 \sin 7\omega t + \cdots + V_n \sin nwt) \qquad (1.1b)$$

The motor current (is I_{rms}) will be

$$I_{rms}{}^2 = I_s{}^2 + \sum I_m \qquad (1.2)$$

In the above equation (1.2),m=3,5,7……, I_m is the harmonic current, I_s is the fundamental current. The interaction of each harmonic currents will results in pulsating torques. The pulsating torque frequency may result in sever vibration, causing fatigue, wearing of gear teeth and unsatisfactory performance in the open loop and closed loop control systems. Core losses are also increased by harmonics and hence the efficiency will be reduced due to increase in losses. Therefore it is mandatory these harmonics should be eliminate or reduced from the output voltage of voltage source inverter (VSI).

1.3 Need for Pulse Width Modulation

Pulse Width Modulation (PWM) strategies are required for switching the devices in a VSI and appropriately to generate adjustable voltage and frequency. Therefore, the switching device in VSI requires optimal pulse pattern and it determines the performance. High performance voltage and current regulators are critical parts of an inverter drive to achieve the task. Depending on the performance requirements, the types of regulators are opted.

In practical applications PWM technique is one among the widely used techniques in voltage source inverters. These inverters are capable of producing ac voltages of variable magnitude as well as variable frequency. The quality of output voltage can be enhanced, when compared with square wave inverters. The PWM inverters are very commonly used in adjustable speed drives where the need of variable voltage, variable frequency supply. For wide variation in drive speed, the frequency of the applied ac voltage needs to be varied over a wide range. The applied voltage also needs to vary almost linearly with the frequency. PWM inverters can be of single phase as well as three phase types.

There are several different PWM techniques, differing in their methods of implementation. However in all these techniques, the aim is to generate an output voltage, which after some filtering, would result in a good quality sinusoidal voltage waveform of desired fundamental frequency and magnitude. In the inverter topology it may not be possible to reduce the overall voltage distortion due to harmonics, but by proper switching control the magnitude of lower order harmonic voltages can be reduced, often at the cost of increasing the magnitudes of higher order harmonic voltages. Such a situation is acceptable in most cases as the harmonic voltages of higher frequencies can be satisfactorily filtered using lower sizes of filter chokes and capacitors. Many of the loads, like motor loads have an inherent quality to suppress high frequency harmonic currents and hence an external filter may not be necessary.

The voltage source inverter employs switching devices with finite turn-on and turn-off characteristics. The amount of switching loss is directly proportional to the transition time taken from turn-on to turn-off and vice-versa. Therefore switching transients strongly affect the energy efficiency, size and reliability of an inverter. Therefore the selection of modulation method plays major role [1]-[4].

Generally the PWM techniques are classified on the basis of voltage or current control, feed-forward or feedback methods, carrier or non carrier based control 1.Sinusoidal PWM 2.Selected harmonic elimination PWM 3.Hysteresis band current control PWM,4.Minimum ripple current PWM, 5.Delta modulation, 6. Sigma-delta modulation, 7.Random PWM 8.Sinusoidal PWM with instantaneous current control 9.Space-vector PWM

Among all these techniques sinusoidal PWM and Space-vector PWM methods are the most popular approaches to real time PWM. The space-vector PWM is an advanced, computation intensive and best among all the PWM techniques for variable voltage and frequency applications. Because of its superior performance characteristics, it has been finding widespread applications in recent years.

1.4 Sinusoidal Pulse Width Modulation

In sinusoidal pulse width modulation the width of each pulse is varied in proportional to the amplitude of sine wave evaluation at the center of the same pulse. In this technique distortion factor and lower order harmonics can be reduced partially. A high frequency triangular wave called the carrier wave is compared to a sinusoidal signal representing the desired output reference wave [12]-[13]. Whenever the carrier wave less than the reference wave is compared and produces a high output signal, which turns on the upper devices in one leg of the inverter on the lower device is off. In the other case the comparator sets the firing signal low which turns the lower switch is on and the upper switch off. The typical wave forms are shown in Fig.1.2 and the modulation index can be find out and which is denoted as M

$$M_{triangle} = \frac{\text{Magnitude}_{\text{reference}}}{\text{Magnitude}_{\text{carrier}}} \tag{1.3}$$

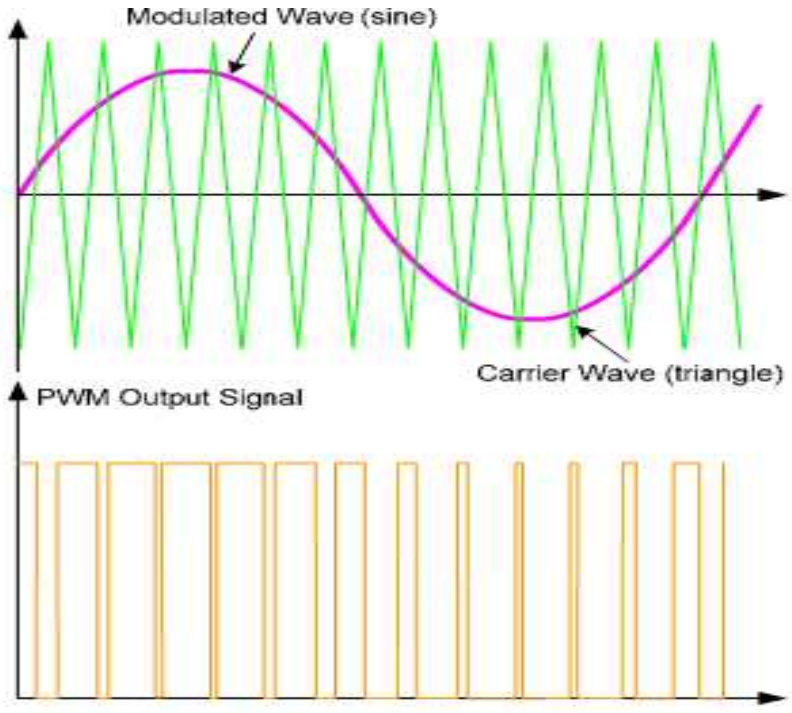

Figure 0.2 SPWM Waveform Generation

The maximum output voltage amplitude obtained with the approach is $0.5V_d$ as $M_{triangle}$may not exceed unity. By applying rectangular square wave on one inverter leg the fundamental voltage is $\frac{4}{\Pi} * 0.5 * V_d = \frac{2}{\Pi} * V_d$ this mode is known as six step entails increased harmonic distortion. It follows that only 78.5% of the inverter capacity is used with sinusoidal modulation. In addition a separate modulation has to be used for each of the inverter legs generating three reference signals forming a balanced three phase system.

In the SPWM comparing a sinusoidal reference signal with triangular carrier wave of frequency (f_c) generated the gating signals. The frequency of reference signal (f_r) determines the inverter output frequency (f_o) and its peak amplitude (A_r) controls the modulation index M and then in turn the RMS output voltage Vo. The number of pulses per half cycle depends on carrier frequency. This is the most popular and commonly used, but suffers from draw backs like low fundamental output voltage and modulation index. By using space vector pulse width modulation technique those drawbacks are over come and improve the fundamental output voltage and also increasing the modulation index.

1.5 Space-Vector PWM

The three phase inverter has eight switching states, six active states and two zero states. These six active vectors divides the space vector plane into six sectors, two zero vectors leads to zero voltage vector. The reference vector has a constant magnitude and revolves with a constant frequency at steady state. A fundamental cycle is divided into several small sub-cycles. By using space vector approach, pulses with variable duty cycle will be generated. The Space-vector PWM technique is complex and switching frequency is limited. The proposed hybrid space vector PWM technique can significantly increase the switching frequency and improved harmonic performance.

1.6 Proposed Hybrid Space Vector PWM

Voltage source inverter fed induction motor is widely used in variable speed applications. Even though PWM varies the speed of the motor efficiently, but it produces harmonics in the line voltage. The deleterious effects of the harmonics on the motor can be enlisted as follows [5], [9]-[11].

- Torque pulsation in the motor due to frequencies of different harmonic order

- Increase in the core losses due to the higher peak flux densities
- Increase the stator winding loss, rotor cage loss and stray load loss due to the additional harmonic currents.
- Increase in the peak current due to the additional current ripples results in the increased loss.

Thus newer PWM technique must aim at reducing this harmonic distortion in the motor line current. A real challenge in the generation of PWM wave form is to minimization of the harmonic distortion in the line current along with the simultaneous reduction of switching loss in the inverter. The proposed hybrid PWM technique based on space vector approach which results in reduced torque ripples and improved switching loss performance[12]-[26]. The main focus of this work will be on the reduction of harmonics distortion in the low and medium power motors. The harmonic distortion in the motor line currents must be low for satisfactory operation of the motor drive [10]. The harmonic distortion in the current is determined by switching frequency and employed PWM technique. The switching frequency cannot be increased beyond certain range due to practical limitations.

This thesis focuses on the development of new real time modulation technique for voltage source inverter. The sinusoidal PWM and space vector PWM (continuous) techniques are very popular for real time environment even though both techniques have own merits and demerits. Space vector PWM (continuous) lead to higher line side voltage for given dc bus voltage compared to sinusoidal PWM, this will results less harmonic distortion in the motor current than sinusoidal PWM. The space vector PWM (discontinuous) leads to reduced distortion at higher line side voltage over a space vector PWM (continuous) for a given switching frequency.

The proposed new hybrid space vector PWM (HSVPWM) is combination of continuous and discontinuous modes of space vector PWM. The HSVPWM explores novel switching sequence and brings out all such possible sequences [13], [17], [21]-[26]. The multiplicity of possible switching sequence provides a choice in the selection of switching sequence in the every sub cycle and finally the proposed hybrid PWM technique employed lowest torque ripples over a given sub cycle, out of given set of sequences.

1.7 Over view of the Thesis

Here the hybrid space vector PWM used in VSI fed induction motor shown in fig 1.3. The hybrid space vector PWM generator takes the frequency and voltage inputs and signals the inverter to switch. DC voltage is converted back to AC by the inverter which supplies energy directly to the induction motorThe HSVPWM minimizing the rms torque ripple over comparable real time space vector PWM at a given switching frequency. It was implemented in MATLAB/SIMULINK.

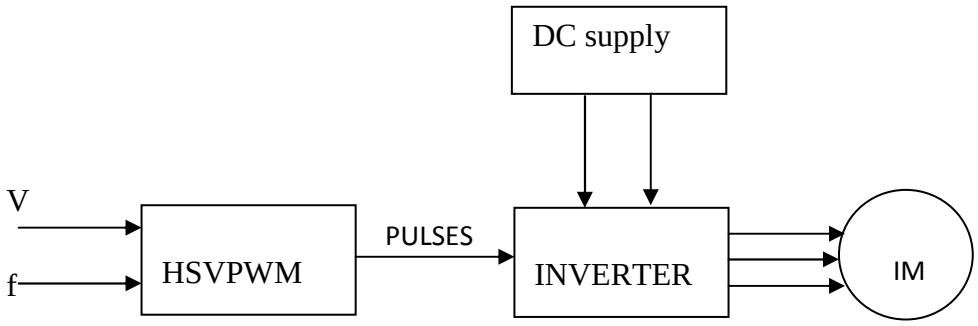

Figure 0.3V/f Control of an Induction Motor Using HSVPWM

CHAPTER -2

SPACE VECTOR BASED PULSE WIDTH MODULATION

2.1 Introduction

The ac voltage is defined by two characteristics namely amplitude and frequency. Hence it is essential to work out an algorithm that permits control over both these quantities. Pulse width modulation controls the average output voltage over a sufficient small period called sampling period by producing pulse of variable duty. By using space vector approach we can get pulses with variable duty cycle [1]-[3], [12]-[15] [29], [31].

2.2 Voltage Space Vector

Three vectors can be represented by one vector which has x-axis component and y-axis component is defined as space vector.

Here the three vectors are defined as 3-phase voltages ofv_a, $v_b, and\ v_c$

Now space vector is

$$v_s = (v_a + v_b e^{j2\pi/3} + v_c e^{-j2\pi/3}) \quad (2.1)$$

When we substitutev_a, v_b, v_c in the equation 2.1 we get

$$v_s = \left(\frac{3}{2}\right) * v_m\,(sin\omega t - jcos\omega t) \quad (2.2)$$

So v_s is having a magnitude of 3/2 and is rotating with frequency of ω as shown in equation (2.2)

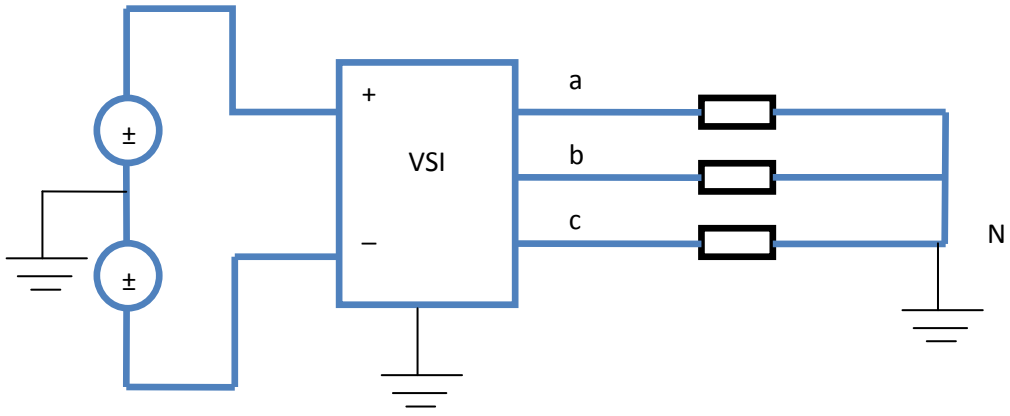

Figure 0.1 Inverter Showing Pole, Line, Phase Voltages

The space vector can also be represented as shown by equation (2.3)

$$v_s = (2/3) * (v_{a0} + v_{b0} e^{j2\pi/3} + v_{c0} e^{j4\pi/3}) \quad (2.3)$$

Here $v_{ao,}\, v_{bo,}\, v_{co}$ are the pole voltages of an inverter as shown in Fig.2.1. In this figure v_{ao}, v_{bo}, v_{co} are the pole voltages and v_{aN}, v_{bN}, v_{cN} are the phase voltages. At any instant in the inverter the pole voltages may be $+\frac{V_{dc}}{2}$ and $-\frac{V_{dc}}{2}$ for an input voltage of V_{dc}, by substituting the pole voltages in the equation (2.3) the $v_s = (2/3)\, V_{dc}$

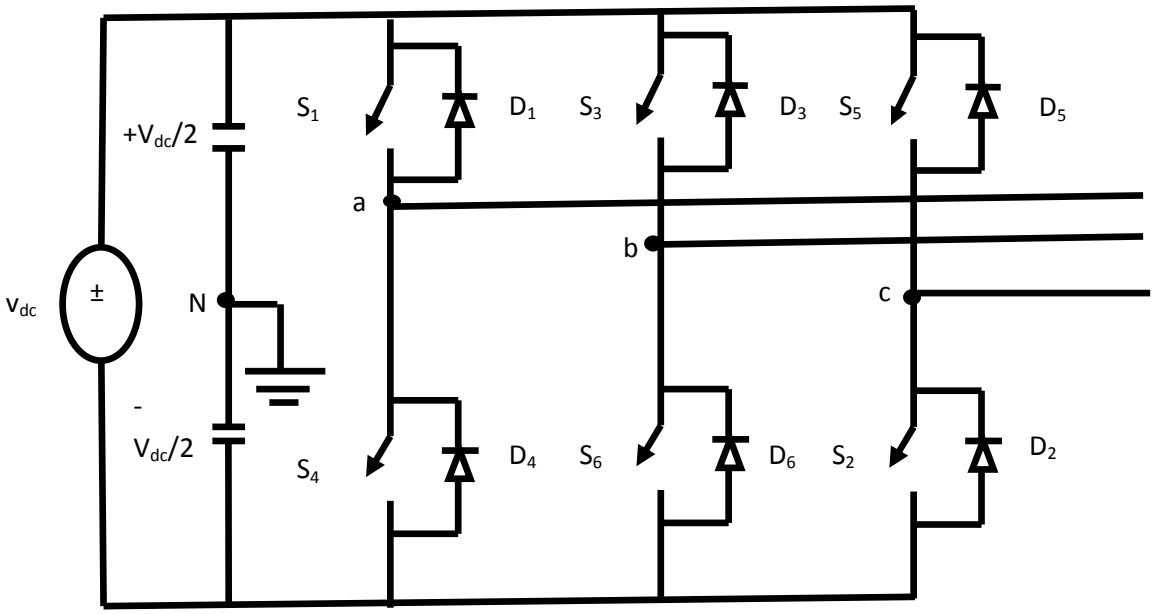

Figure 0.2 Three Phase Voltage Source Inverter

The circuit model of a typical three-phase voltage source PWM inverter is shown in Fig.2.2 S_1 to S_6 are the six power switches that shape the output, which are controlled by the switching VariablesS_1 to S_6. When an upper device is switched on, i.e., when S_1, S_3 or S_5 is **1**, the corresponding lower device is switched off, i.e., S_2, S_4 or S_6 is **0.** Therefore, the ON and OFF states of the upper devices S_1, S_3 and S_5 can be used to determine the output voltage.

As illustrated in Fig. 2.3 there are eight possible combinations of ON and OFF patterns for the three upper power switches. The ON and OFF states of the lower power devices are opposite to the upper one and so they are easily determined once the states of the upper devices are determined.

Table 2.1 Switching vectors, phase voltages and output line to line voltages

Voltage Vectors	**Switching vectors**			**Line to neutral voltage**			**Line to line voltage**		
	a	b	c	V_{an}	V_{bn}	V_{cn}	V_{ab}	V_{bc}	V_{ca}
$\mathbf{V_0}$	0	0	0	0	0	0	0	0	0
$\mathbf{V_1}$	1	0	0	2/3	-1/3	-1/3	0	1	-1
$\mathbf{V_2}$	1	1	1	1/3	1/3	-2/3	0	1	-1
$\mathbf{V_3}$	0	1	0	-1/3	2/3	-1/3	-1	1	0
$\mathbf{V_4}$	0	1	1	-2/3	1/3	1/3	-1	0	1
$\mathbf{V_5}$	0	0	1	-1/3	-1/3	2/3	0	-1	1
$\mathbf{V_6}$	1	0	1	1/3	-2/3	1/3	1	-1	0
$\mathbf{V_7}$	1	1	1	0	0	0	0	0	0

The eight switching vectors, output line to neutral voltage (phase voltage), and output line-to-line voltages in terms of DC-link V_{dc}, are given in Table-2.1 and Fig.2.3 shows the eight inverter voltage vectors (V_0 to V_7).

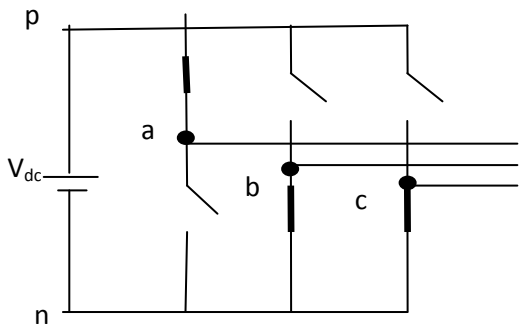

V_1 (100)

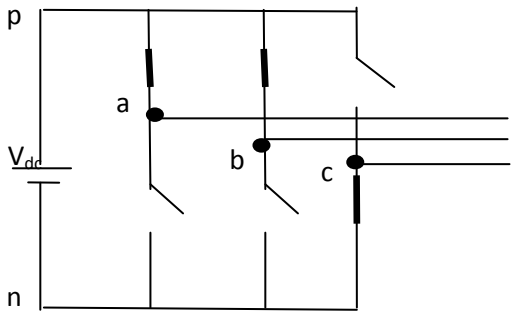

V_2 (110)

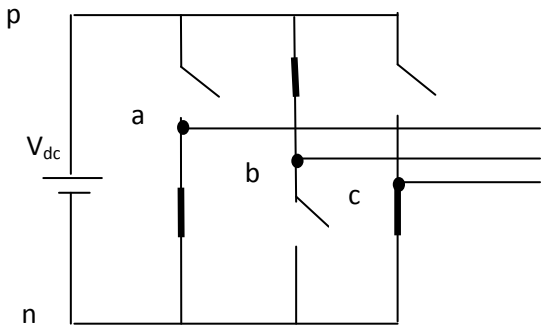

V_3 (010)

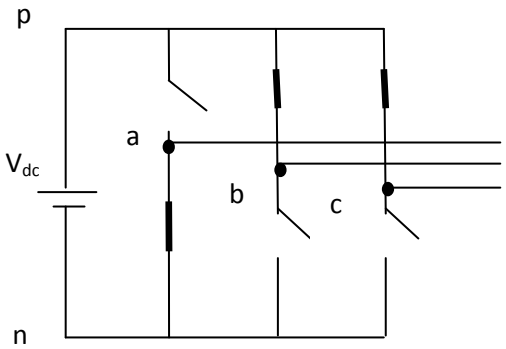

V_4 (011)

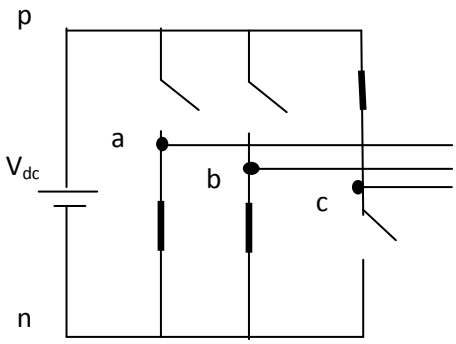

V_5 (001)

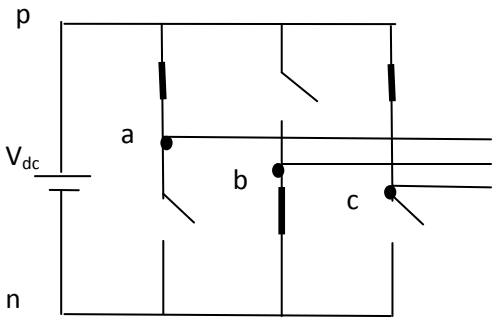

V_6 (101)

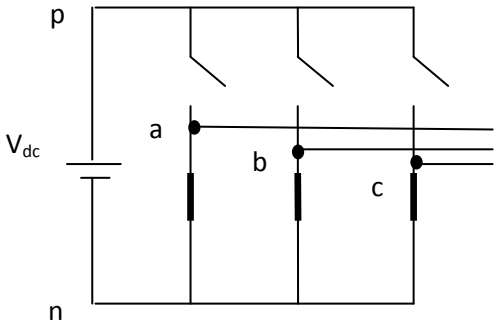

V_0 (000)

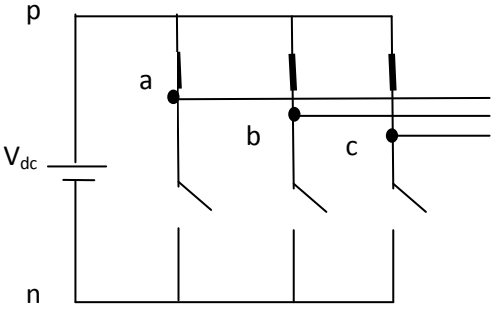

V_7 (111)

Figure 0.3 The Eight Inverter Voltage Vectors (v_0 to v_7)

To implement the space vector PWM, the voltage equations in the *abc* reference frame can be transformed into the stationary *d-q* reference frame that consists of the horizontal (d) and vertical (q) axes. As a result, six non-zero vectors and two zero vectors are possible [12]-[15]. Six nonzero vectors ($V_1 - V_6$) shape the axes of a hexagonal as depicted in Figure 2.4 and feed electric power to the load. The angle between any adjacent two non-zero vectors is 60 degrees. Mean while, two zero vectors (V_0 and V_7) are at the origin and apply zero voltage to the load. The eight vectors are called the basic space vectors and are denoted by V_0, V_1, V_2, V_3, V_4, V_5, V_6, and V_7. The same transformation can be applied to the desired output voltage to get the desired reference voltage vector V_{ref} in the d-q plane.

The objective of space vector PWM technique is to approximate the reference voltage vector V_{ref} using the eight switching patterns. One simple method of approximation is to generate the average output of the inverter in a small period (T) to be the same as that of V_{ref} in the same Period.

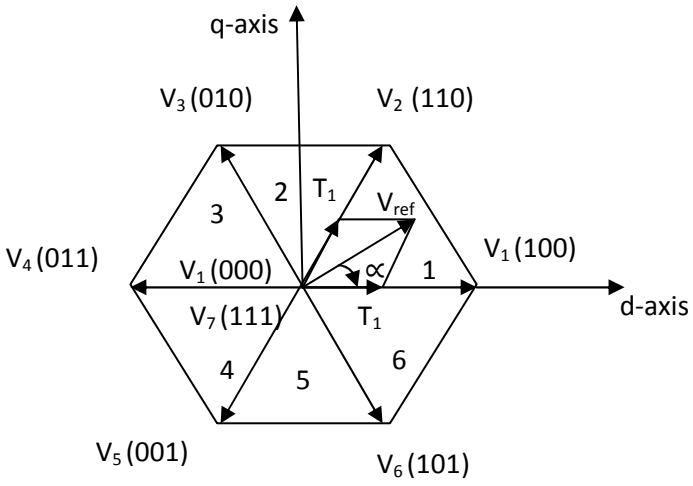

Figure 0.4 Basic switching vectors and Sectors

Then space vector PWM can be implemented by the following steps:

Step 1. Determine V_d, V_q, V_{ref}, and angle (α)

Step 2. Determine time duration T_1, T_2, T_0

Step 3. Determine the switching time of each switching device (S_1 to S_6)

2.3 Determine V_d, V_q, V_{ref}, and angle (α)

The 3-phase sinusoidal voltages are given in equation

$$v_a = v_m \sin(\omega t) \tag{2.6}$$

$$v_b = v_m \sin(\omega t - 120^0) \tag{2.7}$$

$$v_c = v_m \sin(\omega t - 240^0) \tag{2.8}$$

The corresponding 2-phase sinusoidal voltage components are given in equation (2.11)

$$v_d = v_a - \frac{1}{2}(v_b + v_c) \tag{2.9}$$

$$v_q = \frac{\sqrt{3}}{2}(v_b + v_{c)} \tag{2.10}$$

$$V_{ref} = \sqrt{{v_d}^2 + {v_q}^2} \tag{2.11}$$

Angle (α) =$\tan^{-1}\left(\frac{v_q}{v_d}\right)$ (2.12)

2.4 Determine time duration T_1, T_2 and T_z

It is observed that space vector is rotating with frequency ω at any instant the space vector lies in between any two active vectors. Space vector is synthesized by using active vectors and zero vectors [12]-[14].If space vector lies in between any two active vectors , then the two active vectors and zero vector are used to synthesize V_{ref}. PWM technique maintains the balance between the reference and applied volt-seconds over every sub cycle T_s.

Let V_1 be applied for T_1 and V_2 for T_2 and zero vector for T_z

From volt-second balance condition

$$V_{ref..}T_s = V_1 T_1 + V_2 T_2 + V_z T_z \tag{2.13}$$

Zero vector V_z having magnitude zero, by substituting $V_z = 0$ in the equation (2.13)

$$V_{ref..}T_s = V_1 T_1 + V_2 T_2$$

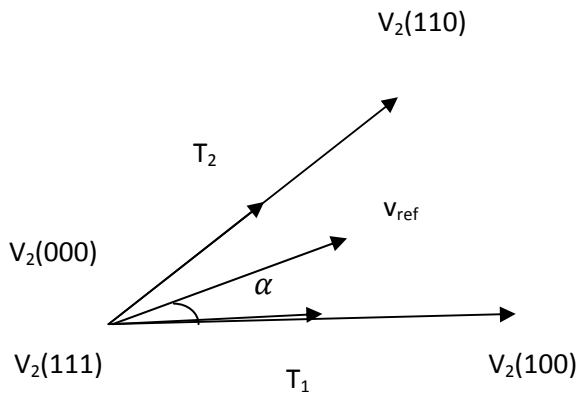

Figure 0.5 Reference Vector as a Combination of Adjacent Vectors at Sector 1

By resolving the equation (2.13) into d and q coordinates

$$T_1 = \frac{V_{ref} \sin\left(\frac{\pi}{3} - \propto\right) T_s}{\sin\left(\frac{\pi}{3}\right)} \qquad (2.14a)$$

$$T_2 = \frac{V_{ref} \sin(\propto) T_s}{\sin\left(\frac{\pi}{3}\right)} \qquad (2.14b)$$

$$T_z = T_s - T_1 - T_2 \qquad (2.14c)$$

2.5 Determination switching time of each device

In Fig. 2.5 V_{ref} is in sector 1. The corresponding switching sequence starts from V_0 (0 0 0) ---V_1 (1 0 0) --- V_2 (1 1 0) ---- V_7 (1 1 1). The switching time of all the switches S_1-S_6 in different sectors are shown in Fig. 2.6. In the Fig. 2.6 all the 3 phases are conducting at a time and there are 3-switchings per sub cycle.

$$\therefore T_s = 1/(2*f_s)$$

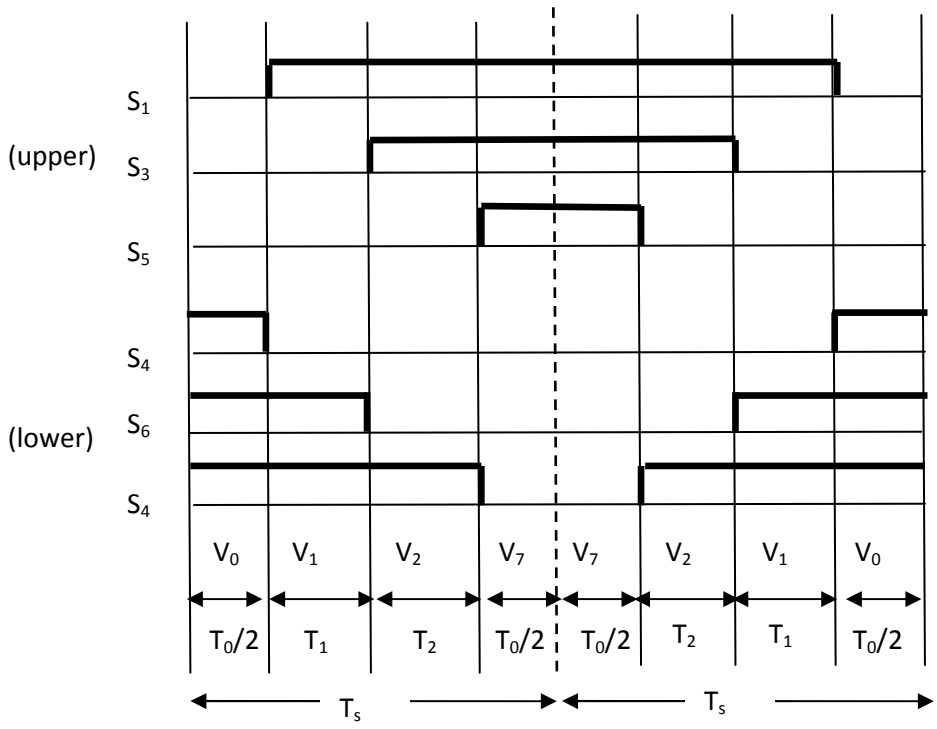

(a) Sector 1

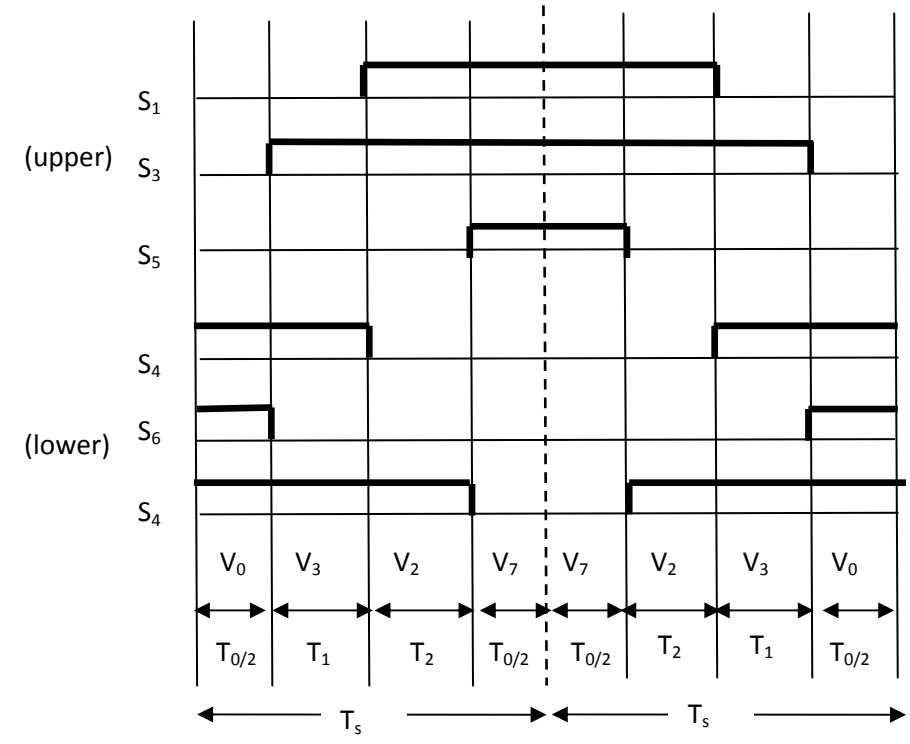

(b) Sector 2

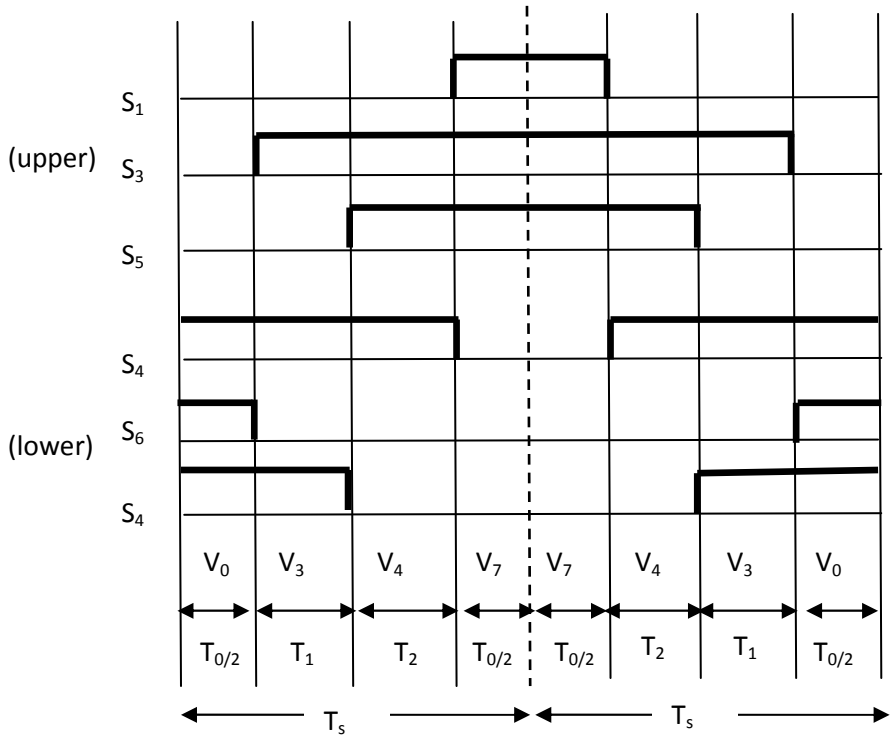

(c) Sector 3

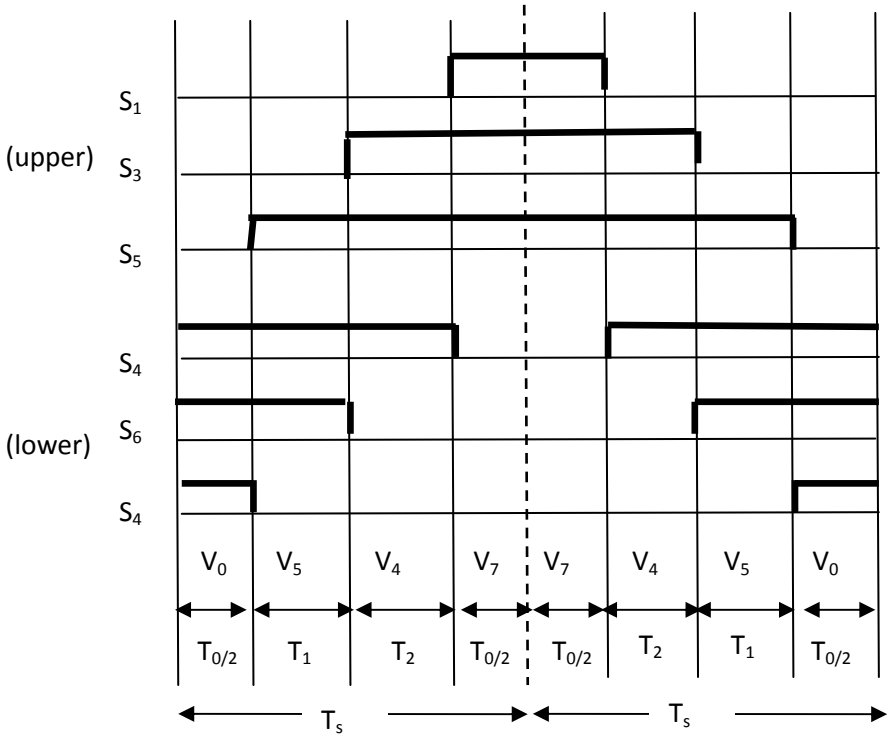

(d) Sector 4

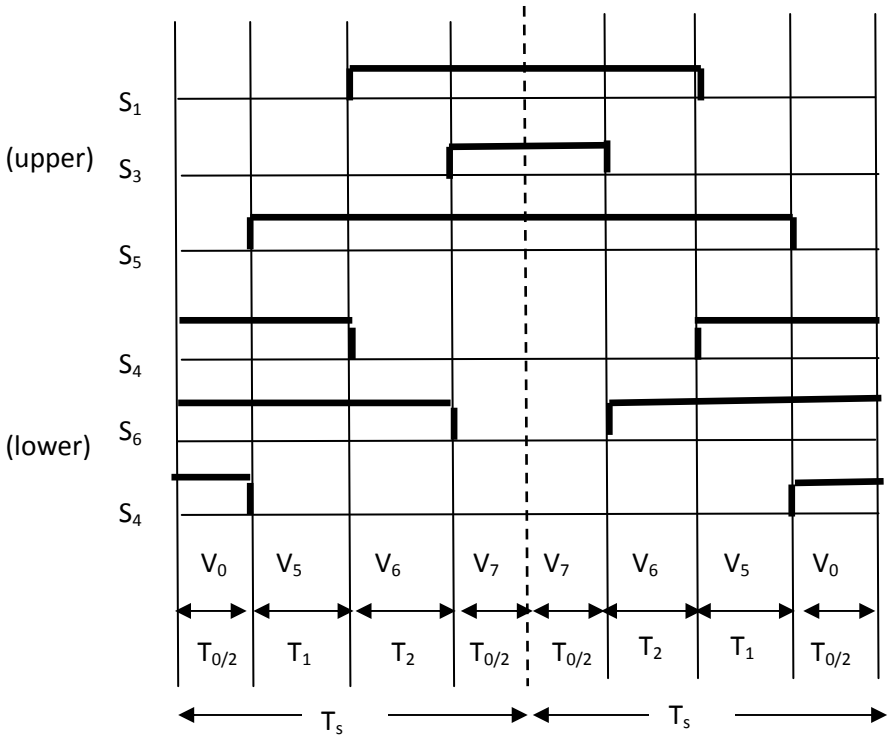

(e) Sector 5

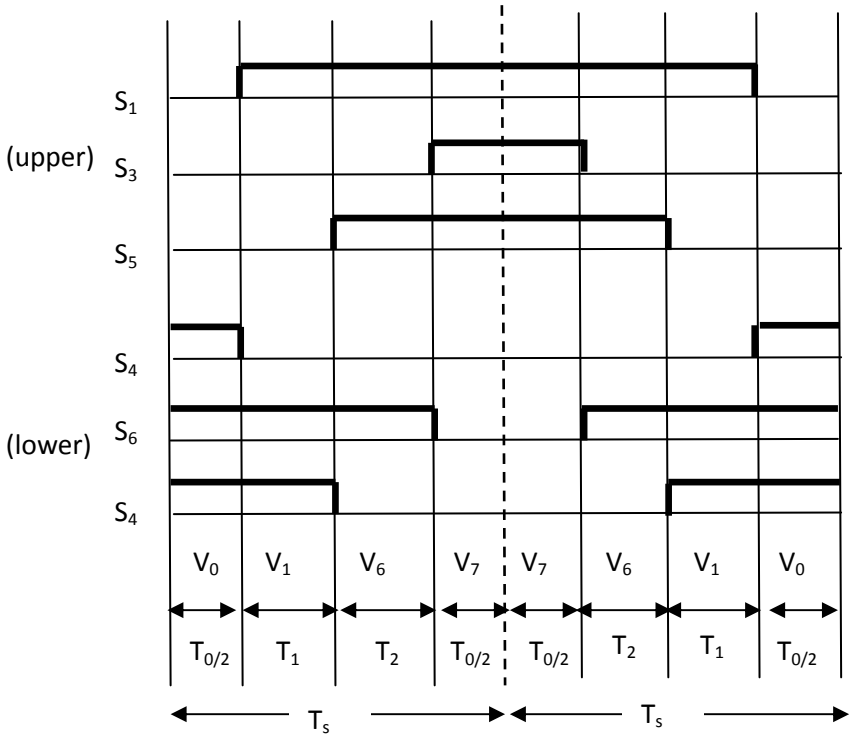

(f) Sector 6

Figure 0.6 Space Vector PWM Switching Patterns at Each Sector

Table-2.2 Switching Time Calculation at Each Sector

Sector	Sequence	Upper switches	Lower switches
1	0127	$S_1 = T_1 + T_2 + T_0/2$ $S_3 = T_2 + T_0/2$ $S_5 = T_0/2$	$S_4 = T_0/2$ $S_6 = T_1 + T_0/2$ $S_2 = T_1 + T_2 + T_0/2$
2	0327	$S_1 = T_1 + T_0/2$ $S_3 = T_1 + T_2 + T_0/2$ $S_5 = T_0/2$	$S_4 = T_2 + T_0/2$ $S_6 = T_0/2$ $S_2 = T_1 + T_2 + T_0/2$
3	0347	$S_1 = T_0/2$ $S_3 = T_1 + T_2 + T_0/2$ $S_5 = T_2 + T_0/2$	$S_4 = T_1 + T_2 + T_0/2$ $S_6 = T_0/2$ $S_2 = T_1 + T_0/2$
4	0547	$S_1 = T_0/2$ $S_3 = T_1 + T_0/2$ $S_5 = T_1 + T_2 + T_0/2$	$S_4 = T_1 + T_2 + T_0/2$ $S_6 = T_2 + T_0/2$ $S_2 = T_0/2$
5	0567	$S_1 = T_2 + T_0/2$ $S_3 = T_0/2$ $S_5 = T_1 + T_2 + T_0/2$	$S_4 = T_1 + T_0/2$ $S_6 = T_1 + T_2 + T_0/2$ $S_2 = T_0/2$
6	0167	$S_1 = T_1 + T_2 + T_0/2$ $S_3 = T_0/2$ $S_5 = T_1 + T_0/2$	$S_4 = T_0/2$ $S_6 = T_1 + T_2 + T_0/2$ $S_2 = T_2 + T_0/2$

Taking switching pattern of each switch in different sectors modulating wave is generated. When this modulating wave is compared with ramp signal, then pulses for upper 3 switches can be generated, for lower switches exactly opposite pulses given because both switches in one leg cannot turn at same time. Therefore for the sequence 0127 the pulse generation is similar to triangle comparison approach as in sine PWM technique but the modulating wave is different in both cases because SVPWM has low THD when compared to sine PWM technique.

CHAPTER-3

NEW SEQUENCES INVOLVING DIVISION OF ACTIVE STATE DURATION

3.1 Introduction

As discussed in the previous chapter, implementation of space vector based PWM with sequence 0127, there are many other sequence which can be used to reduce current ripple and torque ripple. Conventional sequence is 0127 in this two active vectors and two zero vectors are used to represent V_{ref}. CSVPWM divides T_z equally between 0 and 7, and employs the switching sequence 0-1-2-7 or 7-2-1-0 in a sub cycle in sector 1. However, a multiplicity of sequences are possible since the zero vector can be applied either using 0 or 7, and also an active state can be applied more than once in a sub cycle [12], [23], [24]. This project explores and brings out all possible valid switching sequences, which have three switching's per sub cycle as in CSVPWM. The conditions to be satisfied by a valid sequence in sector 1 are as follows.

(i) The active state 1 and the active state 2 must be applied at least once in a sub cycle

(ii) Either the zero state 0 or the zero state 7 must be applied at least once in a sub cycle.

(iii) In case of multiple application of an active state, the total duration for which the active state is applied in a sub cycle must satisfy (i).

(iv) The total duration for which the zero vectors (either using the zero state 0 or the zero state 7) are applied in a sub cycle must satisfy (i).

(v) Only one phase must switch for a state transition.

(vi) The total number of switching's in a sub cycle must be less than or equal to three.

Conditions (i) to (iv) ensure volt–second balance. Condition (v) avoids unwanted switching's to keep the switching losses low. Condition (vi) ensures that the average switching frequency is less than or equal to that of CSVPWM for a given sampling frequency.

The applied inverter state is 0, 1, 2 or 7 at any arbitrary instant in sector 1. The state at the start of a sub cycle, or the initial state, can be any of these four states. Considering 0 to be the initial state, all possible sequences satisfying conditions (i) to (vi) are illustrated in Fig. 3.1(a). Only such sequences that result in exactly three switching's in a sub cycle are considered in Fig.3.1 Sequences 0121 and 0127 are valid sequences, while sequence 0101 is invalid since active state 2 never gets applied [violation of condition (i)]. Similarly, all possible sequences with 1, 2, and 7 as the initial states have been brought out in Fig. 3.1(b)–(d), respectively. Totally ten valid sequences emerge from Fig. 3.1, which can be grouped into five pairs of sequences, namely (0127, 7210),

(0121, 1210), (1012, 2101), (2721, 1272), and (7212, 2127). CSVPWM uses the pair of conventional sequences (0127, 7210) in alternate sub cycles in sector 1. The other four pairs can also be employed in alternate sub cycles in sector 1. These four pairs of sequences are termed as "special sequences," since these result in double-switching of a phase, single switching of another phase and clamping of the third phase in the given sub cycle. In special sequences of type I, there are two transitions between the active states 1 and 2. In special sequences of type II, there are two transitions between an active state and the zero state closer to it (i.e., between 1 and 0 or between 2 and 7). Further there are also valid sequences with only two switching's, namely 012, 210, 721, 127. Sequence 012, for instance, can be viewed as a special case of 0127, 0121, or 1012. Similarly, the other two-switching sequences can also be seen as special cases of certain three-switching sequences. These sequences are termed as "clamping sequences," and are employed by discontinuous modulation methods [12]-[24]. Sequences 012 and 210 or sequences 721 and 127 can be used in alternate sub cycles in sector 1. All the above sequences pertain to sector 1. Sequences pertaining to the other sectors are listed in Table-3.1

Table-3.1 Switching sequence in six sectors

Sector	**Convectional sequence**	**Type –II sequence**	**Type-III sequence**	**Type-IV Sequence**
1	0127-7210	012-210 721-127	0121-1210 7212-2127	1012-2101 2721-1272
2	0327-7230	032-230 723-327	0323-3230 7232-2327	3032-2303 2723-3272
3	0347-7430	034-430 743-347	0343-3430 7434-4347	3034-4303 4743-3474
4	0547-7450	054-450 745-547	0545-5450 7454-4547	5054-4505 4745-5474
5	0567-7650	056-650 765-567	0565-5650 7656-6567	5056-6505 6765-5676
6	0167-7610	016-610 761-167	0161-1610 7616-6167	1016-6101 6761-1676

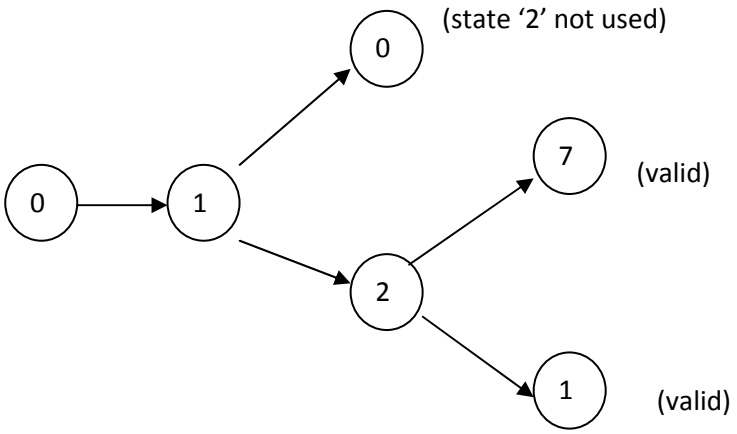
0
(state ‘2’ not used)
0
1
7
(valid)
2
1
(valid)

(a)

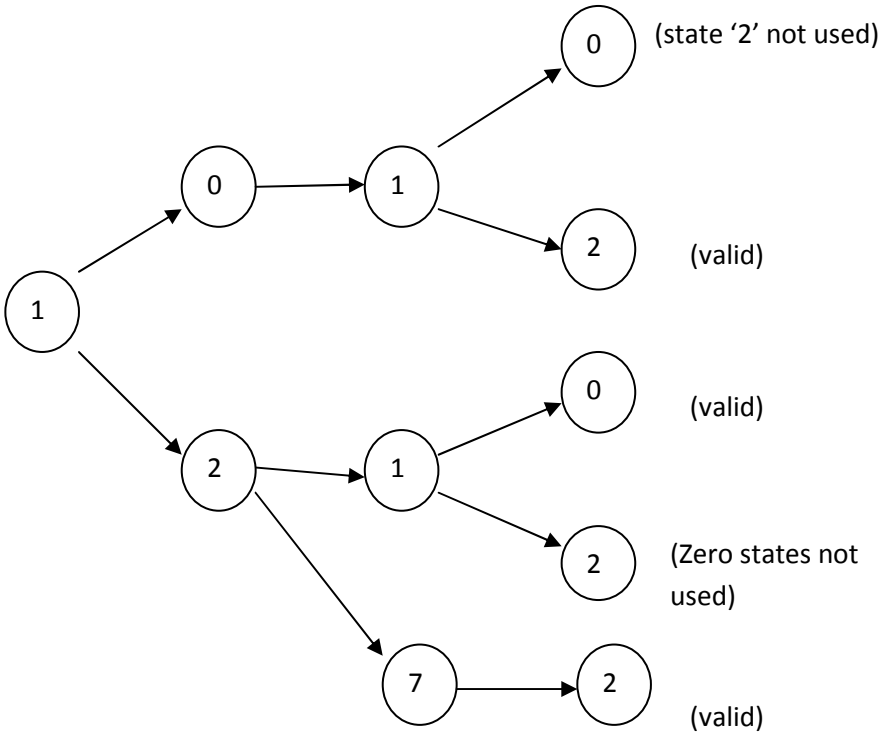
0
(state ‘2’ not used)
0
1
2
(valid)
1
0
(valid)
2
1
2
(Zero states not used)
7
2
(valid)

(b)

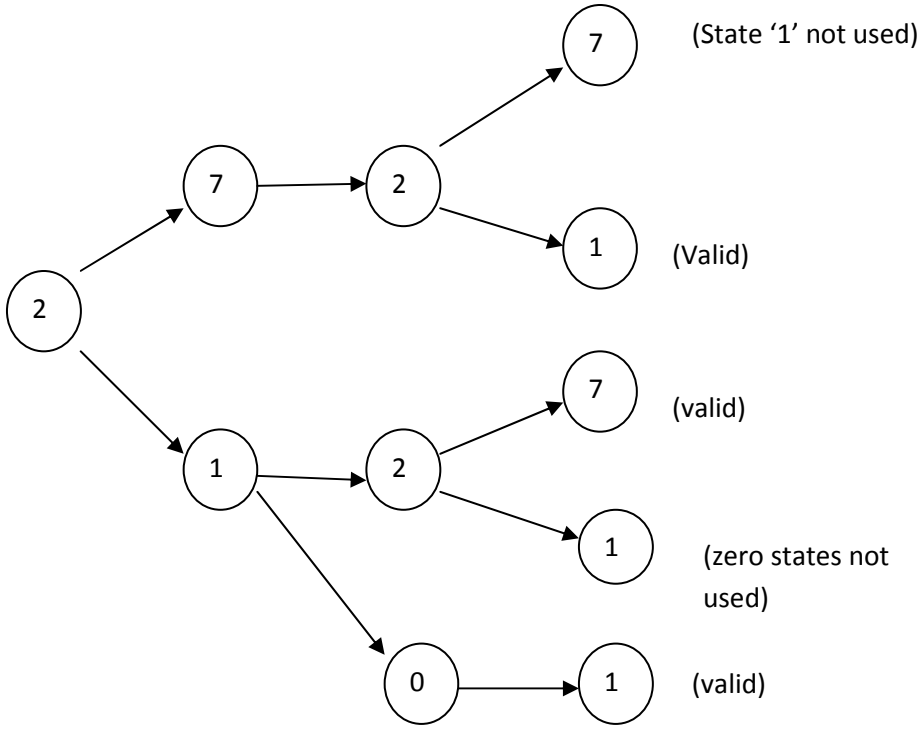

(c)

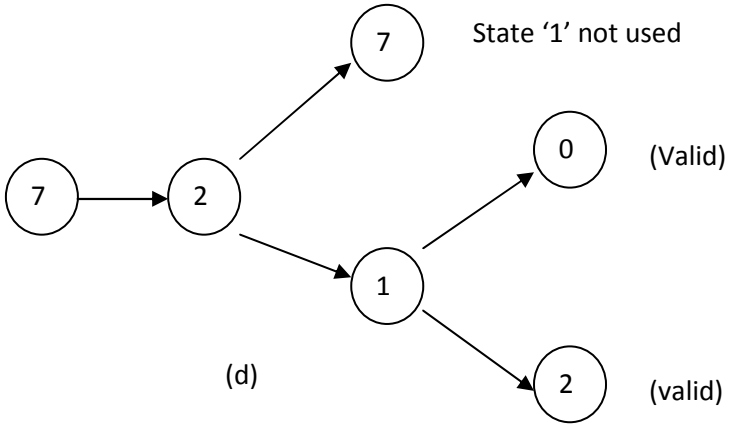

(d)

Figure 0.1 Valid sequences for initial state (a) 0, (b) 1, (c) 2, And (d) 7.

Fig. 3.1 shows the derivations of all possible sequences that have three switching's per sub-cycle and satisfy the above constraints. For example, starting from state 0 in Fig 3.1a, the only possibility for the next state is 1, since states 2 or 7 will

involve multiple switching's. From state 1, through transition to state 0 is possible, it will rule out the use of state 2, and hence is not a valid sequence. Therefore the next state has to be 2. From state 2, transitions to either state 1 or state 7 involve only one switching and hence both are allowed. This leads to two sequences the conventional sequence 0127 and the new sequence 0121, which involves division of the duration of active state 1. Following a similar procedure all the possible sequences with the above mentioned constrains can be derived as illustrated in Fig. 3.1.

3.2 Sequence 012

The implementation of SVPWM technique with other sequence carried out by taking one zero vector instead of two zero vectors as in conventional SVPWM. The sequence possible is 012 and 721. For the sequence 012 calculating V_{ref}, angle (α), sector and times T_1, T_2 and T_z is same as conventional SVPWM. The switching time for different switches changes with different sequences. The difference between convection SVPWM based sequence and 012 sequence is that two switching's per sub cycle is present in 012 sequence (i.e. 0--1-2) but in 0127 three switching's per sub cycle is present (i.e. 0-1-2-7). Hence for a given average switching frequency the sub cycle duration is reduced to two third for the sequences 012 when compared with the sequence 0127. This reduced sub cycle duration could lead to reduced RMS torque ripple and RMS current ripple at high values of V_{ref} [17], [20]-[23].

Therefore

$T_s=1/(2f_s)$ for 0127

$T_s=1/(3f_s)$ for 012

$T_s=1/(3f_s)$ for 721

The switching time of switches S_1, S_3, S_5 is shown in Fig.3.2 for sector1. It can be generalized for remaining sectors.

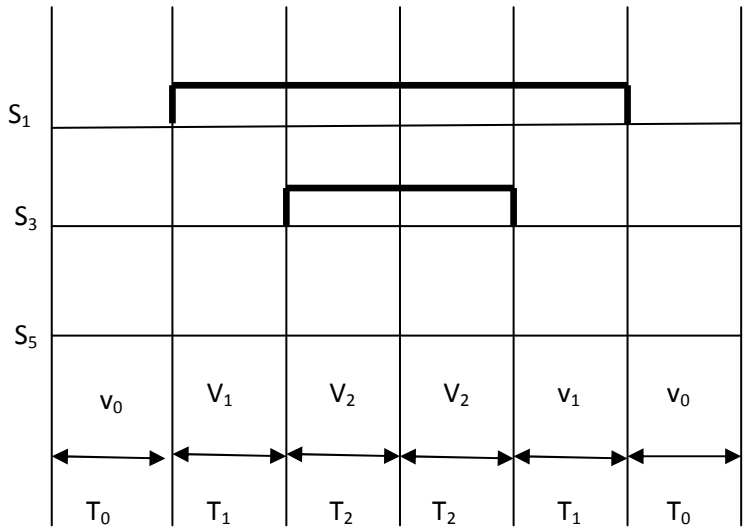

Figure 0.2 Switching Pattern of Sequence 012 for Sector-1

From the Fig.3.2 it can be observed that only 2-phases conduct at a time the other phase is clamped. There will be 120^0 clamping for sequence 012.The switching pattern in different sectors for all the switches (S_1-S_6)is given in the table-3.2 in terms of T_1, T_2,T_0.

Table-3.2 Switching Time Calculation at Each Sector for the **012** type sequence

Sector	Sequence	Upper switches	Lower switches
1	012	$S_1 = T_1 + T_2$ $S_3 = T_2$ $S_5 = 0$	$S_4 = T_0$ $S_6 = T_1 + T_0$ $S_2 = T_1 + T_2 + T_0$
2	032	$S_1 = T_1$ $S_3 = T_1 + T_2$ $S_5 = 0$	$S_4 = T_2 + T_0$ $S_6 = T_0$ $S_2 = T_1 + T_2 + T_0$
3	034	$S_1 = 0$ $S_3 = T_1 + T_2$ $S_5 = T_2$	$S_4 = T_1 + T_2 + T_0$ $S_6 = T_0$ $S_2 = T_1 + T_0$
4	054	$S_1 = 0$ $S_3 = T_1$ $S_5 = T_1 + T_2$	$S_4 = T_1 + T_2 + T_0$ $S_6 = T_2 + T_0$ $S_2 = T_0$
5	056	$S_1 = T_2$ $S_3 = 0$ $S_5 = T_1 + T_2$	$S_4 = T_1 + T_0$ $S_6 = T_1 + T_2 + T_0$ $S_2 = T_0$
6	01	$S_1 = T_1 + T_2$ $S_3 = 0$ $S_5 = T_1$	$S_4 = T_0$ $S_6 = T_1 + T_2 + T_0$ $S_2 = T_2 + T_0$

By taking above switching pattern in different sectors modulating wave can be generate which has a clamping of 120^0 in each phase. This modulating wave is similar to the sequence 0127 clamping in each phase. This modulating wave compared with ramp signal SVPWM pulses will be generated; these pulses will be given to the switches S_1 to S_6. Therefore this method is also similar to triangular comparison approach. The only difference modulating wave has 120^0 clamping.

3.3 Sequence 1012

The implementation of SVPWM technique with other sequence is carried out by dividing active vector in to two equal halves instead of dividing zero vectors in to two equal halves as in conventional SVPWM. The sequence possible is 1012.This sequence 1012 comes under type III sequence. In this sequence there will be three switching's per sub cycle same as 0127 sequence but the difference is that only two phases conduct at a time i.e. 120^0 clamping in the each phase.

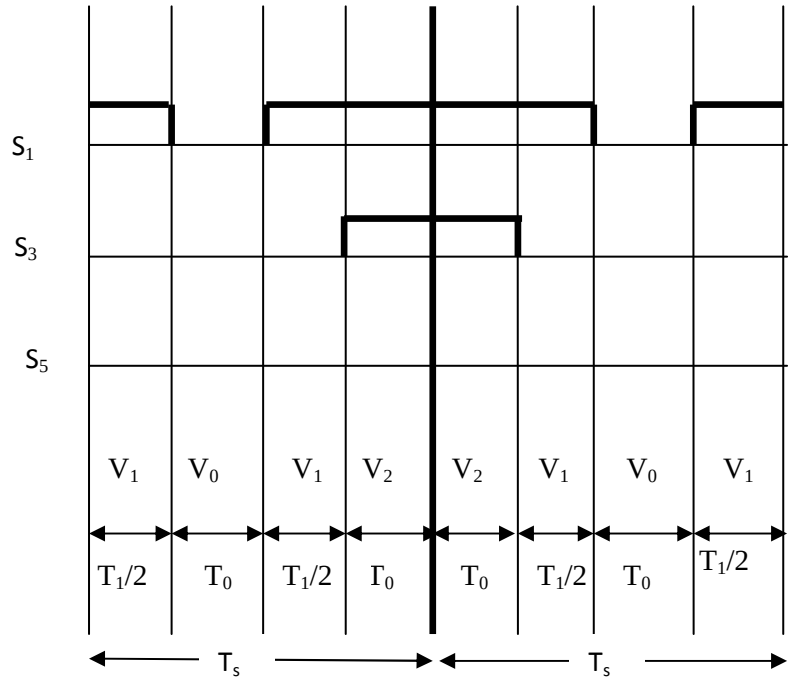

Figure 0.3 Switching Pattern of Sequence 1012 for Sector-1

In this sequence calculating V_{ref}, alpha (α), sector, T_1, T_2, and T_z same as 0127 sequence but switching time is different for different switches in different sectors. The switching time of switches S_1, S_3, S_5 are shown in Fig.3.3 for sector1. It can be generalized for remaining sectors.

In the Fig.3.3 phase A double switches, phase B single switching and phase C is clamped within the sub cycle. So that clamping in each phase is 120^0. There are 3 switching's per sub cycle therefore

$$T_s=1/(2f_s).$$

The switching pattern for all the switches (S_1-S_6) for 1012 sequence is given in the table-3.3 below in terms of T_1, T_2 ,T_0.

Table-3.3 Switching Time Calculation for the **1012** sequence

sector	**sequence**	**Upper switches**	**Lower switches**
1	1012	$S_1 = T_1 + T_2$ $S_3 = T_2$ $S_5 = 0$	$S_4 = T_0$ $S_6 = T_1 + T_0$ $S_2 = T_1 + T_2 + T_0$

In the two cases 012 and 1012 the switching pattern is same for both sequences as shown in table –3.2 and table-3.3.

CHAPTER-4

ANALYSIS OF CURRENT RIPPLE OVER A SUB-CYCLE

4.1 Derivation of flux ripple

In the previous chapter, it was explained implementation of SVPWM pulses with different SVPWM based sequence. In the space vector approach the applied voltage vector is equal to the reference voltage vector. The zero voltage vector and active voltage vector are forming the boundary in a sector and were used to generate this reference voltage vector. The instantaneous voltage ripple vector for a sampled positioned in the sector-1 corresponding to the active vector 1, active vector 2, and zero vector are as shown in Fig.4.1. In this, when there is a switching, the applied voltage vector is changed instantaneously hence the voltage ripple vector is changed between any two consecutive switching instants the applied voltage vector remains the same. As the reference voltage vector keeps revolving the voltage ripple vector also changes continuously w. r. t. time both in magnitude as well as angle.

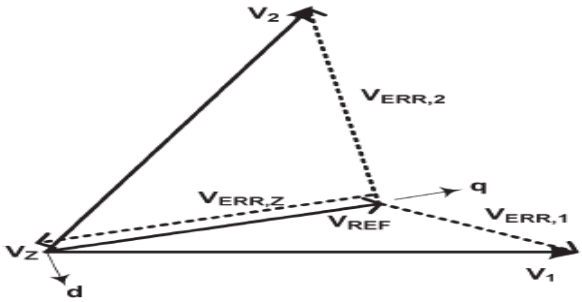

Figure 0.1 Error voltage vectors corresponding to active vector 1, active vector 2 and zero vector

The voltage ripple vectors can be represented in a synchronously revolving d-q axis reference as shown in Fig.4.1. The q-axis is in the direction of the reference voltage vector while the d-axis is 90^0 behind the q-axis. The instantaneous voltage ripple vector in the synchronously revolving d-q reference frame corresponding to the active voltage vectors 1, 2 and the zero voltage vector are given in equations (4.1).

$$V_{rip1} = \frac{2}{3}V_{dc}sin\alpha + j\left(\frac{2}{3}\,V_{dc}cos\alpha - V_{ref}\right) \tag{4.1a}$$

$$V_{rip2} = -\frac{2}{3}V_{dc}\sin(60-\alpha) + j\left(\frac{2}{3}V_{dc}\cos(60-\alpha) - V_{ref}\right) \tag{4.1b}$$

$$V_{ripz} = -jV_{ref} \tag{4.1c}$$

The time integral of the voltage ripple vector is referred as the stator flux ripple vector and is a measure of ripple in the line current at any instant within a sub cycle. In each sub-cycle one of the two active voltage vectors or the zero voltage vectors is

applied. When the zero voltage vector is applied, the error voltage vector is equal to the negative of the average vector to be generated. When an active vector is applied the voltage ripple vector originating from the tip of the reference voltage vector and ending at the tip of the active voltage vector applied.

As the voltage ripple vector remains constant, the ripple flux voltage changes at a uniform rate for any applied vector. The application of a zero voltage vector results in a variation of the q-axis component of the flux ripple, but the application of any active voltage vector results in variation of both the d-axis and q-axis components [18], [20], [23], [24]. The error volt-second quantities are given by equation (4.2).

$$V_{rip1} * T_1 = \frac{2}{3} V_{dc} * T_1 sin\alpha + j\left(\frac{2}{3} V_{dc} cos\alpha - V_{ref}\right) * T_1$$

$$= D_1 + jQ_1 \quad (4.2\ a)$$

$$V_{rip2} * T_2 = -\frac{2}{3} V_{dc} * T_2 \sin(60 - \alpha) + j\left(\frac{2}{3} V_{dc} \cos(60 - \alpha) - V_{ref}\right) * T_2$$

$$= D_2 + jQ_2 \quad (4.2\ b)$$

$$V_{ripz} = -jV_{ref} * T_Z$$

$$= jQ_z \quad (4.2\ c)$$

Where

$$D_1 = \frac{2}{3} V_{dc} T_1 sin\alpha \quad (4.3\ a)$$

$$D_2 = \frac{2}{3} V_{dc} * T_2 \sin(60 - \alpha) \quad (4.3\ b)$$

By substituting T_1 and T_2 expression in the equation 4.3

$D_1=D_2$

Therefore $D_1=D_2=D$.

$$Q_1 = \left(\frac{2}{3} V_{dc} cos\alpha - V_{ref}\right) * T_1 \quad (4.4\ a)$$

$$Q_2 = \left(\frac{2}{3} V_{dc} \cos\left(\frac{\pi}{3} - \alpha\right) - V_{ref}\right) * T_2 \quad (4.4\ b)$$

$$Q_z = -V_{ref} * T_Z \quad (4.4\ c)$$

The sum of equations (4.4) equated to zero, which indicates the balance between applied volt-seconds and reference volt-seconds over a sub cycle. The volt –second balance ensures that the stator flux ripple vector starts and ends with zero magnitude in

every sub cycle. The variation in between these zero instants is a measure of the harmonic distortion in the 3-phase current. This variation depends on the reference voltage generated and switching sequence used.

4.2 Variation of stator flux ripple over a sub cycle

The trajectory of the stator flux ripple vector tip is along the direction of the ripple voltage vector, as stator flux ripple vector is time integral of voltage ripple vector. The Fig 4.1 shows the variation of the stator flux ripple vector over a sub cycle for seven possible switching sequence for a given reference voltage vector. The corresponding d-axis and q-axis stator flux ripple vectors are also shown. The q-axis stator flux ripple at the switching instants is given in terms of Q_z, Q_1 and Q_2 while those d-axis stator flux ripple are given in terms of D. The quantities Q_z, Q_1, Q_2 and D are defined in equations 4.3 and 4.4.

The tip of the stator flux ripple vector for conventional SVPWM (0127 - sector 1) sequence has the triangular trajectory over a sub cycle as shown in Fig. 4.2.

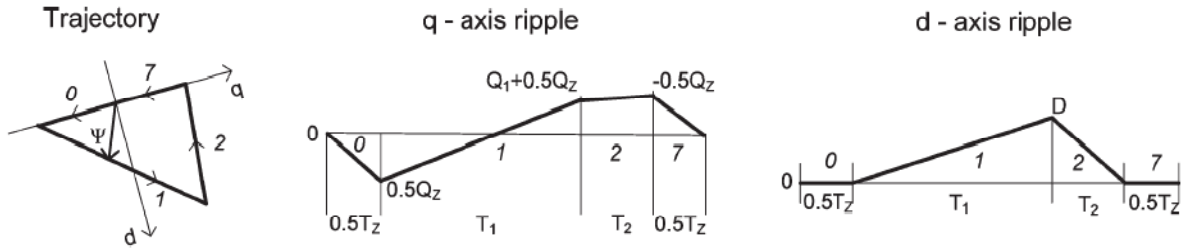

Figure 0.2 Stator Flux Ripple Corresponding To Sequence 0127 over a Sub Cycle

The stator flux ripple vector for the sequence 012 and 721 is shown in Fig.4.3

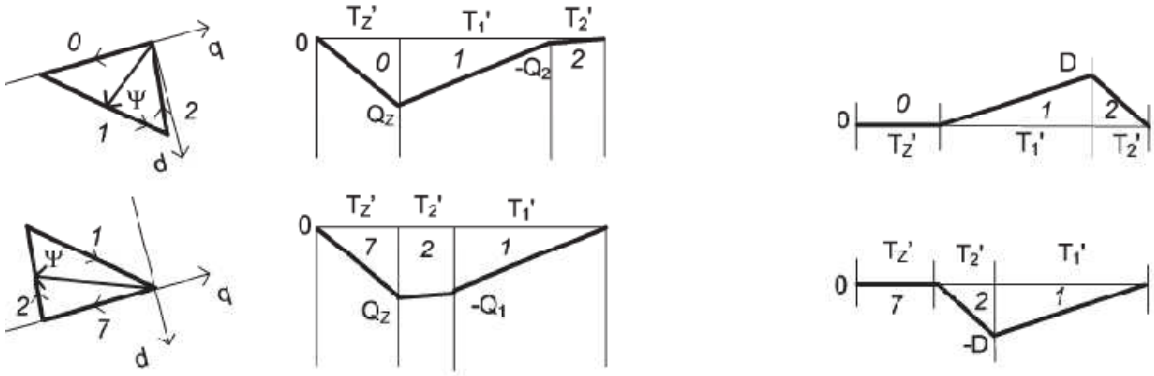

Figure 0.3 Stator Flux Ripple Corresponding To Sequence 012 And 721 Over A Sub Cycle

The stator flux ripple tip trajectory is triangular which was same as conventional sequence and was shown in Fig.4.3 for the sample considered in the first half of the sector 1. The mean square value of the d-axis ripple was equal for the both the sequences, but it was not so with q-axis ripple. As The q-axis component does not change appreciably when the active state 2 is applied, for the sequence 721 the q-axis ripple continued to remain fairly high through-out the duration of state 2 and decreased only when state 1 was applied. Thus the mean square ripple is high for the sequence 721 than that of 012.

Conversely if the sample is in the second half of the sector 1 then the sequence 721 will result in lesser ripple than 012. In general when a clamping sequence is used, to minimize the mean square ripple, the active vector sample must precede or succeeded by a zero vector and there must be only one switching at any instant, so appropriate zero state must be selected.

The stator flux ripple vector in the case of the sequence 0121 and 7212 are shown in Fig. 4.4. The stator flux ripple trajectories in these two cases form a double triangle as shown in fig 4.4. The switching sequence 0121 performs better than that of 7212 in the first half of the sector-1. Conversely if the sample is in the second half of the sector–1 then the sequence 7212 will result lesser ripple than 0121. Thus the pair of complementary switching sequences are

(i) 012 and 721

(ii) 0121 and 7212

(iii) 1012 and 2721

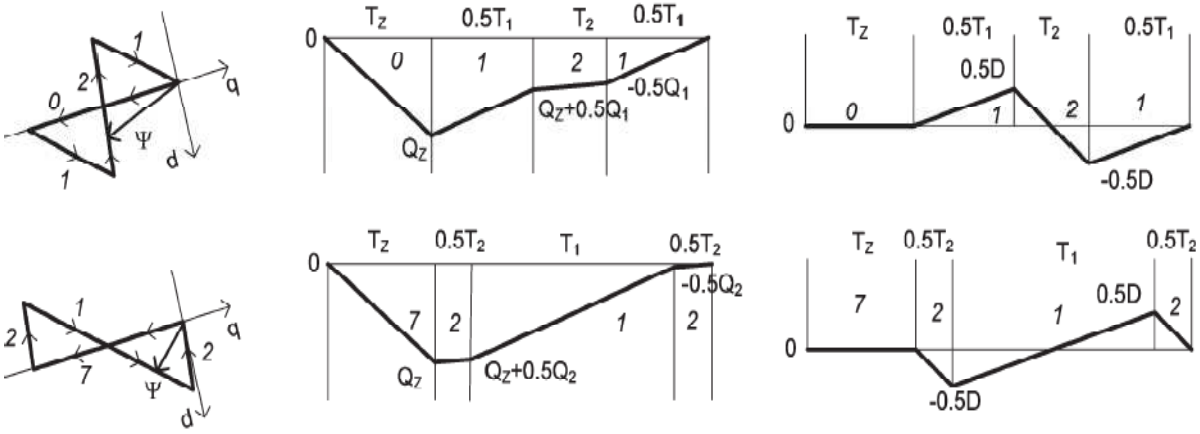

Figure 0.4 Stator Flux Ripple Corresponding To Sequence 0121 And 7212 Over A Sub Cycle

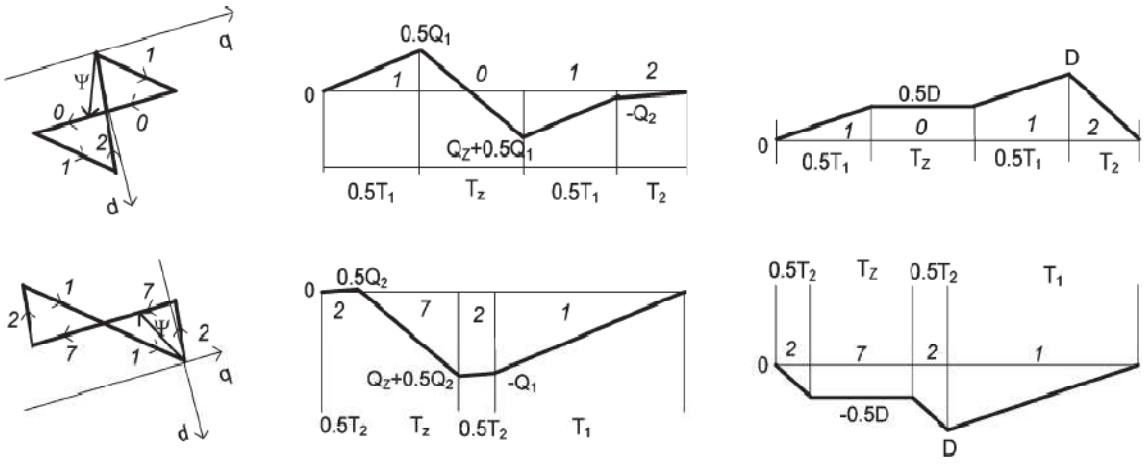

Figure 0.5 Stator Flux Ripple Corresponding To Sequence 1012 And 2721 Over A Sub Cycle

The RMS stator flux ripple over a sub cycle corresponding to a sequence is denoted by F_{seq} (where seq= 0127, 012, 721, 1012 and 2721). The expression for the mean square ripple can be derived in terms of Q_z, Q_1, Q_2 and D. The stator flux ripple is resolved into its component along the d-axis and q-axis. The d-axis ripple and q-axis ripple for 0127 switching sequence are given in equation (4.7).

$$\Psi_{q(0127)} = \frac{Q_z t}{T_z} \quad \text{if } 0 < t < 0.5Tz \tag{4.5 a}$$

$$= 0.5Q_z + \frac{Q_1 t_1}{T_1} \quad if \quad 0.5\,T_z \leq t \leq (0.5T_z + T_1) \tag{4.5 b}$$

$$= 0.5Q_z + Q_1 + \frac{Q_2 t_2}{T_2} \quad if \quad (0.5T_z + T_1) \leq t \leq (T_s - 0.5T_z) \tag{4.5c}$$

$$= 0.5Q_z + \frac{Q_z t_3}{T_z} \quad if \quad (T_s - 0.5T_z) \leq t \leq T_s \tag{4.5 d}$$

$$\Psi_{d(0127)} = 0 \quad \text{If } 0 < t < 0.5Tz \tag{4.6 a}$$

$$= \frac{Dt_1}{T_1} \quad if \quad 0.5\,T_z \leq t \leq (0.5T_z + T_1) \tag{4.6 b}$$

$$= D - \frac{Dt_2}{T_2} \quad if \quad (0.5T_z + T_1) \leq t \leq (T_s - 0.5T_z) \tag{4.6 c}$$

$$= 0 \quad if \quad (T_s - 0.5T_z) \leq t \leq T_s \tag{4.6 d}$$

Where $t_1 = t - 0.5T_z$

$t_2 = t - 0.5T_z - T_1$

$t_3 = t - 0.5T_z - T_1 - T_2$

The mean square stator flux ripple over a sub cycle for the sequence 0127 can be calculated as

$$F^2{}_{0127} = \frac{1}{T_s}\int_0^{T_s} \Psi^2{}_{d(0127)}\, dt + \frac{1}{T_s}\int_0^{T_s} \Psi^2{}_{q(0127)}\, dt$$

$$\begin{aligned} F^2_{0127} = {} & \frac{1}{3}(0.5Q_Z)^2 T_Z/2T_S + \frac{1}{3}\left[(0.5Q_Z)^2 + 0.5Q_Z(0.5Q_Z + Q_1) + (0.5Q_Z + Q_1)^2\right]\frac{T_1}{T_S} \\ & + \frac{1}{3}\left[(0.5Q_Z + Q_1)^2 - 0.5Q_Z(0.5Q_Z + Q_1) + (-0.5Q_Z)^2\right]\frac{T_2}{T_S} \\ & + \frac{1}{3}(-0.5Q_Z)^2 T_Z/2T_S + 1/3D^2(T_1 + T_2)/T_S \end{aligned} \quad (4.7)$$

$$\begin{aligned} F^2_{012} = {} & \frac{1}{3}(Q_Z)^2 T_Z/T_S + \frac{1}{3}\left[Q_Z^2 + Q_Z(Q_Z + Q_1) + (Q_Z + Q_1)^2\right]\frac{T_1}{T_S} + \frac{1}{3}\left[(Q_Z + Q_1)^2\right]\frac{T_2}{T_S} \\ & + \frac{1}{3}D^2(T_1 + T_2)/T_S \end{aligned} \quad (4.8)$$

$$\begin{aligned} F^2_{721} = {} & \frac{1}{3}(Q_Z)^2 T_Z/T_S + \frac{1}{3}\left[Q_Z^2 + Q_Z(Q_Z + Q_2) + (Q_Z + Q_2)^2\right]\frac{T_2}{T_S} + \frac{1}{3}\left[(Q_Z + Q_2)^2\right]\frac{T_1}{T_S} \\ & + \frac{1}{3}D^2(T_1 + T_2)/T_S \end{aligned} \quad (4.9)$$

$$\begin{aligned} F^2_{1012} = {} & \frac{1}{3}(0.5Q_Z)^2 T_Z/2T_S + \frac{1}{3}\left[(0.5Q_1)^2 + 0.5Q_1(0.5Q_1 + Q_z) + (0.5Q_1 + Q_z)^2\right]\frac{T_z}{T_S} \\ & + \frac{1}{3}\left[(0.5Q_1 + Q_z)^2 + (0.5Q_Z + Q_z)(Q_Z + Q_1) + (Q_Z + Q_1)^2\right]\frac{T_1}{2T_S} \\ & + \frac{1}{3}(Q_Z + Q_1)^2 T_2/T_S + 1/3D^2(T_1 + T_2)/T_S + (0.5D)^2\frac{T_z}{T_S} \end{aligned} \quad (4.10)$$

$$\begin{aligned} F^2_{2721} = {} & \frac{1}{3}(0.5Q_2)^2 T_2/2T_S + \frac{1}{3}\left[(0.5Q_2)^2 + 0.5Q_2(0.5Q_2 + Q_z) + (0.5Q_2 + Q_z)^2\right]\frac{T_z}{T_S} \\ & + \frac{1}{3}\left[(0.5Q_2 + Q_z)^2 + (0.5Q_2 + Q_z)(Q_2 + Q_Z) + (Q_2 + Q_Z)^2\right]\frac{T_1}{2T_S} \\ & + \frac{1}{3}(Q_Z + Q_2)^2 T_1/T_S + \frac{1}{3}D^2(T_1 + T_2)/T_S + (0.5D)^2\frac{T_z}{T_S} \end{aligned} \quad (4.11)$$

Thus the proposed method of analysis is capable of estimating d-axis ripple and q-axis ripple individually. It was observed that the THD of current wave was equally affected by the d-axis and q-axis ripples. On the other hand, torque pulsation is mainly depends on q-axis ripple and independent of d-axis stator flux ripple. Thus the reduced q-

axis ripple signifies the reduction of THD and torque pulsation, while the reduction of d-axis stator flux ripple affects only THD.

From the above observations it can be conclude that for few specified sequences at high modulation index the d-axis ripple is dominant and results in an overall reduction of stator flux ripple but q-axis ripple increases. It shows that at high modulation indices the THD due to bus clamping sequence PWM is better than conventional SVPWM, but moderate increase in torque pulsation due to increase in q-axis ripple. The rms stator flux ripple over a sub cycle depends on the reference vector and the switching sequences employed.

4.3. Optimal continuous modulation

The duration T_z is divided into two zero states 0 and 7, as shown in equation (4.12). While x always equals 0.5 in conventional SVPWM, different continuous and discontinuous modulation methods primarily differ in terms of this fraction x.

$$T_0 = xT_z \qquad (4.12\ a)$$

$$T_7 = (1-x)T_z, \quad 0 \leq x \leq 1 \qquad (4.12\ b)$$

The rms current ripple over a sub-cycle is a function of the fraction x , while the ratio x = 0.5, as in conventional SVPWM, leads to good properties, this is still a suboptimal. The optimal value of x, which results in the minimum rms current ripple over a sub-cycle for the given reference vector, is given by x_{opt} in (4.13)

$$x_{opt} = \frac{T_z+T_2}{2T_s} - \frac{Q_1}{Q_z}\frac{T_1+T_2}{2T_s}, 0 \leq x_{opt} \leq 1 \qquad (4.13)$$

Substituting Q_z, Q_1, T_1, T_2 and T_z in the equation (4.13), the optimal duration for which the zero state 0 must be applied, $T_{0\ (opt),}$ is shown in equation (4.14 a). The zero state 7 must be applied for the remaining fraction of duration T_z, as shown in equation (4.14b).

$$T_{0(opt)} = X_{0pt}T_z \qquad (4.14\ a)$$

$$T_{0(opt)} = T_z - T_{0(opt)} \qquad (4.14\ b)$$

The rms d-axis current ripple over a sub cycle is independent of the fraction x, but the optimal value of x essentially minimizes the rms q-axis current ripple. Consequently, x_{opt}

leads to minimum possible rms torque ripple over the given sub-cycle for the given reference vector.

4.4. Hybrid PWM

With discontinuous modulation, the fraction x is either 1 or 0. If $x = 1$, then the sequence is 012 or 210, where only zero state 0 is used. If $x = 0$, the sequence is 721 or 127, which employs only the zero state 7. Each sequence consists of two switching per sub-cycle. Hence, for a given average switching frequency f_s the sub cycle duration can be reduced to two thirds for these sequences, compared to sequence 0127. The reduced sub cycle duration could lead to reduced rms torque ripple or rms current ripple, particularly for high values of V_{ref} . Therefore, given a reference vector in sector 1 the following three options could be considered in selecting a switching sequence.

1) Sequence 0127, with $x = x_{opt}$ and $T_s = 1/(2\ f_s)$;

2) Sequence 012, with $x = 1$ and $T_s = 1/(3\ f_s)$;

3) Sequence 721, with $x = 0$ and $T_s = 1/(3\ f_s)$.

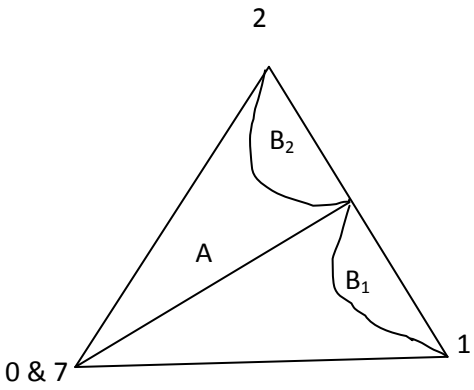

Figure 0.6 Hybrid PWM with 012-721-0127 Sequence

A comparison of the three sequences in terms of rms torque ripple or rms q-axis current ripple over a sub cycle using equations 4.7-4.11 brings out the regions of superior performance of the three, which are shown in Fig.5.2. Sequence 0127, with the active vectors positioned optimally within the sub cycle, leads to the lowest rms torque ripple in region A, as shown in Fig. 4.6. Sequence 012 is better than sequence 721 for $\alpha < 30^\circ$ and vice versa for $\alpha > 30^\circ$. Sequences 012 and 721 are best in regions B1 and B2, respectively, which are symmetric about the center of the sector (i.e., $\alpha = 30^\circ$), as seen in Fig. 4.6.

CHAPTER- 5

SIMULATION AND RESULTS

5.1 Simulation circuit

Circuit diagram for open loop control of induction motor is shown in Fig.5.1 using hybrid PWM technique. The Fig.5.1 contains internal subsystems for both inverter and induction motor.

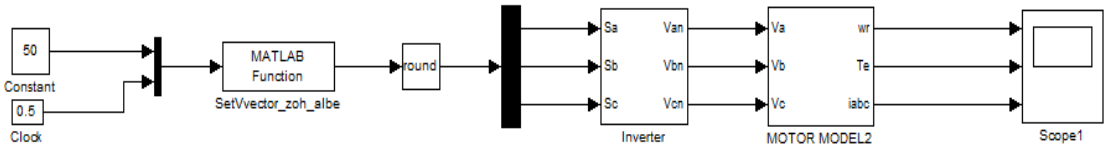

Figure 0.1 Open Loop V/f Control Simulation circuit

.

1.2 V/f control technique

The open loop V/f control method is most popular method of speed control because of simplicity and considered magnetic variation of control variables only this method is also called as scalar control method as shown in fig 5.2 the flux and torque are function of frequency and voltage respectively. The induced voltage in the air gap is

$$E_{ag} = k * \phi_{ag}$$

$$\phi_{ag} = constant = \frac{E_{ag}}{f} = \frac{V}{f}$$

Where ϕ_{ag} is the air gap flux in Weber's

Speed is varied by varying the frequency and maintains V/f constant to avoid saturation of flux. With constant V/f ratio motor develops constant maximum torque i.e. constant torque mode except at low speeds because as the frequency becomes small at low speeds the stator voltage drop comes into picture thus weakening the flux. To over cum this draw back the boost voltage Vo is added so increasing the gain (G=V/f) that the rated flux and corresponding full torque becomes available down to zero speed as shown in Fig.5.2. Here note the effect of boost voltage becomes negligible at high frequency.

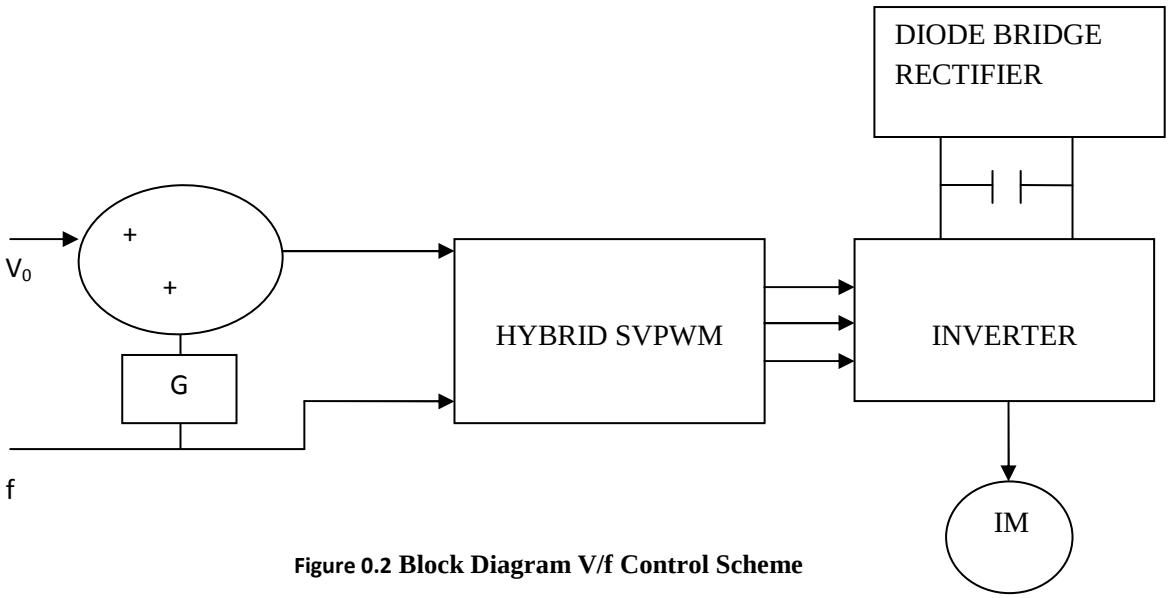

Figure 0.2 Block Diagram V/f Control Scheme

As seen in space vector implementation requires conversion of 3 axis to 2 axis i.e. abc-dq axes, calculating V_{ref}, calculating angle, sector finding, switching times T_1,T_2,T_z calculation, and switching times of all the switches are implemented by coding in MATLAB. From that coding pulses are generated as output. When the pulses are given to inverter and with an input DC voltage AC output voltage is obtained. Modeling of inverter is shown in Fig.5.3

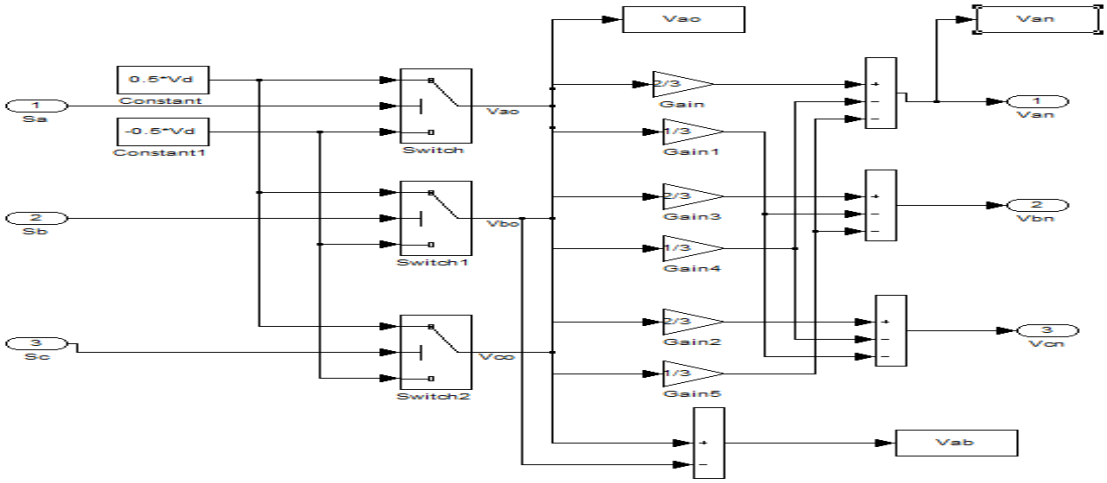

Figure 0.3 Modeling Of Inverter

In the Fig.5.3 S_a, S_b and S_c are the pulses which are given to the phases. We are giving pole voltage as input. The pole voltage is converted into phase voltage. This phase voltage is given as input to the induction motor.

5.3 Simulation results

The torque plots for different sequences are presented here

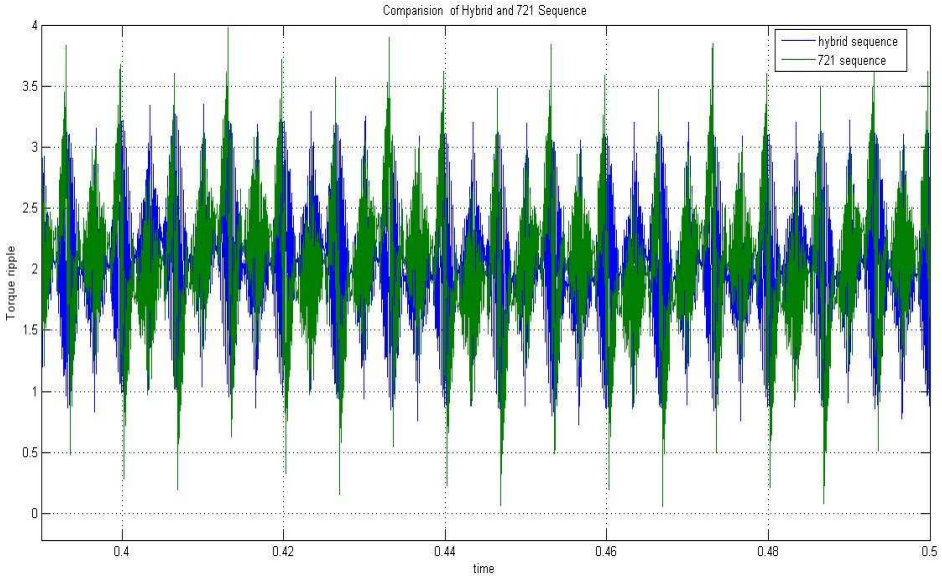

Figure 0.4 Comparison of torque ripple hybrid sequence with 721

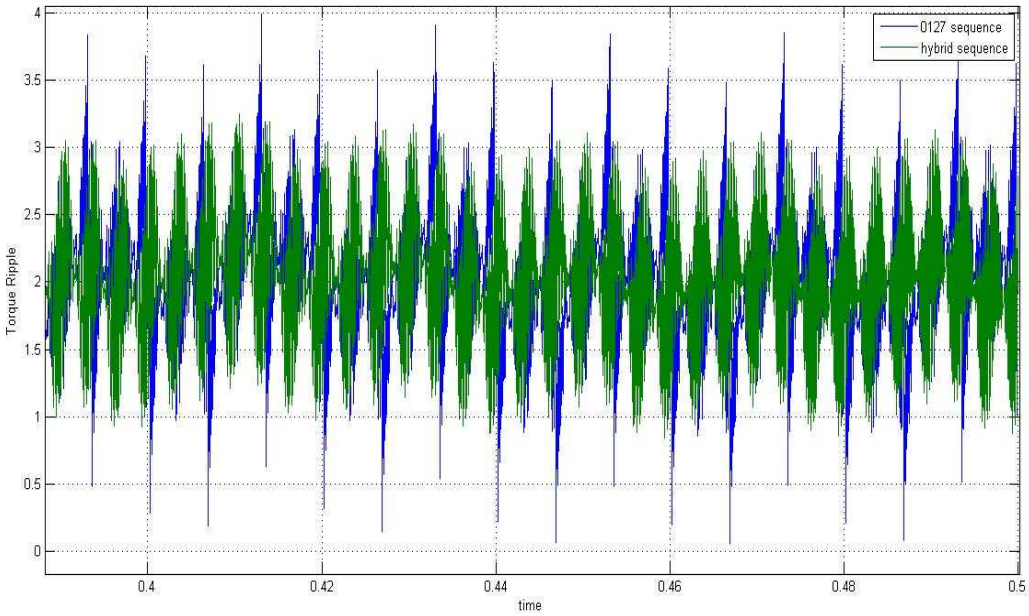

Figure 0.5 Comparison of torque ripple hybrid sequence with 0127

The rms values of current ripple as well as torque ripple are proportional to the sub cycle duration T_s. The normalized rms torque ripple corresponding to the Hybrid PWM is compared against that of CSVPWM (i.e. 0127 sequence) in Fig. 5.5. Similarly, rms torque ripples due to Hybrid PWM and that of bus-clamping PWM method (i.e. 721 sequences) are shown in Fig. 5.4.

5.1 Comparison of torque ripple Hybrid sequence with 0127 sequence and 721

Time	Torque ripple		
	0127 sequence	721 sequence	Hybrid sequence
0.40	2.0853	2.1008	2.0598
0.42	2.1208	2.0903	2.0954
0.44	2.0996	1.9905	1.9992
0.46	1.9920	1.9724	1.9665
0.48	2.0122	1.9878	1.9860
0.5	2.0253	1.9979	1.9994

It can be observed from the table 5.1 the reduction of torque ripple with Hybrid PWM is more than that of bus-clamping PWM and the amount of ripple is less than that of conventional PWM.

CHAPTER -6

CONCLUSION AND FUTURE SCOPE

Conclusion

The space vector approach to generation of PWM waveform offers several advantages over the traditional triangle comparison methods. Novel switching sequences which can be employed in space vector PWM generation are brought out. Influence of the switching sequence on the torque ripple over a sub cycle is investigated. A procedure is presented for designing hybrid PWM technique involving multiple sequences for reduced torque ripple.

The application of advanced bus-clamping switching sequences for torque ripple reduction in induction drives has been studied. A hybrid PWM technique, which is a combination of a conventional sequence and advanced bus-clamping sequences, has been proposed for the reduction of the pulsating torque. However, the conventional sequence 0127 and the existing bus clamping sequences, 012 and 721 in space vector duration, offer additional degree of freedom that are not possible in triangle comparison approach. All possible sequences that involve division of active vector duration, and satisfy constraints similar those of conventional sequences have been identified in this work. With the new sequences , it is possible to realize double switching , single switching or zero switching (clamping) of a phase within a sub-cycle, as appropriate, whereas the conventional sequence always results in just single switching per phase per sub-cycle. The number of pulses per sub-cycle in the line-line voltages is also different when the new sequences are used.

Hybrid PWM technique refers to the use of different sequences in different sub-cycle with in a sector, unlike the conventional PWM, which applies 0127 throughout sector 1. These hybrid techniques result reduction in torque ripples compared to the conventional SVPWM. Simulation results are showing a significant reduction of torque ripple and a marginal improvement in harmonic distortion of line current due to the proposed hybrid PWM method, compared to SVPWM.

Future scope:

Possible future work in this area that show promise of further improvement in the performance of induction motor drives are listed below.

1. In the present study, the active state duration (as well as zero state duration) is divided equally into two intervals, to form new sequences. Unequal division of active vector duration can lead to further improvement in steady state performance.

2. The present study has focused on three- phase, two-level converters, which have only eight states. Multi-level PWM converter has been a subject of vigorous research recently. With a total of n^3 possible states, the multi-level PWM can reduce the THD significantly, though at the expense of increased control complexity. The concept of division of active state duration can be investigated for multi–level converters to achieve improved performance in terms of THD, switching loss and input current ripple.

References

[1] Van der Broeck, H.W., Skudelny, H.C., and Stanke, G.V.: 'Analysis and realization of pulse width modulator based on voltage space vector', IEEE Trans., 1988, IA-24, pp. 142–150

[2] X.Wu, S. K. Panda, and J. Xu, "Effect of pulse-width modulation schemes on the performance of three-phase voltage source converter," in *Proc. 33rd Annu. IEEE IECON*, 2007, pp. 2026–2031.

[3] Wei, S., Wu, B., Li, F., and Liu, C.: 'A general space vector PWM control algorithm for multilevel inverters'. Proc. IEEE Conf. APEC, 2003, pp. 562–568

[4] Celanovic, N., and Boroyevich, D.: 'A fast space vector modulation algorithm for multilevel three phase converters', IEEE Trans., 2001,IA-37, pp. 637–641

[5] V. E. Wagner, et al, "Effects of Harmonics on Equipment," IEEE Trans. on Power Delivery, Vol. 8,No. 2, pp. 672-680, April, 1993.

[6] Shakir M. Abdulrahman, J. G. Kettleborough, and R.Smith, "Fast Calculation of Harmonic Torque Pulsations in a VSI Induction Motor Drive", *IEEE Trans. On Industrial Electronics*, vol. 40, no. 6

[7] IEEE Recommended Practices and Requirements for Harmonics Control in Electrical Power Systems, ANSU IEEE Standard 519, Jan., 1993

[8] D. Casadei, G. Serra, A. Tani, and L. Zarri, "Theoretical and experimental analysis for the RMS current ripple minimization in induction motor drives controlled by SVM technique," *IEEE Trans. Ind. Electron.*, vol. 51,no. 5, pp. 1056–1065, Oct. 2004.

[9] T. H. Ortmeyer, K. R. Chakravarthi and A. A.Mahmoud, "The Effects of Power System Harmonics on Power System Equipment and Loads," IEEE Trans. on Power Apparatus and Systems, Vol. PAS- 104, No. 9, pp. 2555-2563, Sept., 1985.

[10] Ching-Yin Lee; Wei-Jen Lee Effects of Voltage Harmonics on the Electrical and Mechanical Performance of a Three-phase Induction Motor, industrial and commercial power systems conference 1998 IEEE

[11] D. J. Sheppard, "Torsional Vibration Resulting from Adjustable-Frequency AC Drives", *IEEE Trans. On Industry Applications*, vol. 24, no. ***5,*** pp. 812-817,1988.

[12] J. Holtz, "Pulse width modulation—A survey," *IEEE Trans. Ind. Electron.*,vol. 39, no. 5, pp. 410–420, Dec. 1992

[13] S. Ogasawara, H. Akagi, and A. Nabae, "A novel PWM scheme of voltage source inverters based on space vector theory," in *Proc. EPE*, Aachen, Germany, Oct. 1989, pp. 1197–1202.

[14] D. G. Holmes and T. A. Lipo, *Pulse Width Modulation for Power Converters: Principles and Practice*. Piscataway, NJ: IEEE Press, 2003

[15] V. Blasko, "Analysis of a hybrid PWM based on modified space-vector and triangle-comparison methods," *IEEE Trans. Ind. Appl.*, vol. 33, no. 3,pp. 756–764, May 1997

[16] D. Casadei, G. Serra, A. Tani, and L. Zarri, "Theoretical and experimental analysis for the rms current ripple minimization in induction motor drives controlled by SVM technique," *IEEE Trans. Ind. Electron.*, vol. 51, no. 5, pp. 1056–1065, Oct. 2004.

[17] L. Dalessandro, S. D. Round, U. Drofenik, and J. W. Kolar, "Discontinuous space-vector modulation for three-level PWM rectifiers," *IEEE Trans. Power Electron.*, vol. 23, no. 2, pp. 530–542, Mar. 2008

[18] A. Mehrizi-Sani and S. Filizadeh, "An optimized space vector modulation sequence for improved harmonic performance," *IEEE Trans. Ind. Electron.*, vol. 56, no. 8, pp. 2894–2903, Aug. 2009.

[19] K. Taniguchi, M. Inoue, Y. Takeda, and S. Morimoto, "A PWM strategy for reducing torque-ripple in inverter-fed induction motor," *IEEE Trans. Ind. Appl.*, vol. 30, no. 1, pp. 71–77, Jan./Feb. 1994.

[20] K. Basu, J. S. S. Prasad, and G. Narayanan, "Minimization of torque ripple in PWM ac drives," *IEEE Trans. Ind. Electron.*, vol. 56, no. 2, pp. 553–558, Feb. 2009

[21] Kaushik Basu, J. S. Siva Prasad, G. Narayanan Reduction of Torque Ripple in Induction Motor Drives Using an Advanced Hybrid PWM Technique ,IEEE TRANSACTIONS ON INDUSTRIAL ELECTRONICS, VOL. 57, NO. 6, JUNE 2010

[23] G. Narayanan, D. Zhao, H. K. Krishnamurthy, R. Ayyanar, and V. T. Ranganathan, "Space vector based hybrid PWM techniques for reduced current ripple," *IEEE Trans. Ind. Electron.*, vol. 55, no. 4, pp. 1614–1627, Apr. 2008

[24] G. Narayanan and V. T. Ranganathan, "Analytical evaluation of harmonic distortion in PWM AC drives using the notion of stator flux ripple," *IEEE Trans. Power Electron.*, vol. 20, no. 2, pp. 466–474, Mar. 2005

[25] K. Taniguchi, M. Inoue, Y. Takeda, and S. Morimoto, "A PWM strategy for reducing torque-ripple in inverter-fed induction motor," *IEEE Trans. Ind. Appl.*, vol. 30, no. 1, pp. 71–77, Jan./Feb. 1994.

.

[26] Udayar Senthil & **B.** G. Femandes Hybrid Space Vector Pulse Width Modulation Based Direct Torque Controlled Induction Motor Drive

[27] Thomas G. Habetler, et,al, "Direct Torque Control of Induction Machines Using Space Vector Modulation", IEEE Trans. Industrial Applications., Vol. 28, No.5, pp. 1045-1053, September/October 1992.

[28] N. Mohan, T. M. Undeland, and W. P. Robbins, Power Electronics; Converter, Applications and Design, John Wiley and Sons, 2003,

[29] R. S. Lai and K. D. T. Ngo, "A PWM method for reduction of switching loss in a Full-bridge inverter, " IEEE Trans. Power Electronics., vol. 10, pp. 326-332, May 1995

[30] M. H. Rashid, Power Electronics: circuits, devices, and Applications, Pearson Education, 2004

[31] Bimal K. Bose, “Modern Power Electronics and AC Drives” Pearson Education,2003